Reply to acp-2017-167-RC1-supplement, a review of the manuscript ACP-2017-167 “Winds and temperatures of the Arctic middle atmosphere during January measured by Doppler lidar”

Jens Hildebrand et al.

June 26, 2017

The authors present middle atmospheric wind and temperature observations of a lidar system in northern Norway during three Januaries. These observations are compared to the ECMWF and the HWM07 model. Besides the thermal and dynamical mean state, the authors also examine the variability caused by gravity waves and large-scale waves in the observations and the model data.

In a previous review I wrote to the authors “While the collocated middle atmospheric wind and temperature measurements of the Alomar RMR lidar are unique and unprecedented in their temporal and vertical resolution, I find it hard to learn something new from the paper. As it stands right now, the paper is mainly a comparison of different profiles, but no substantial conclusions are drawn from this.” This is still the case. Thus, I can only recommend publication of the article after substantial revisions.

Please find my detailed comments below.

Major comments

1. As said before, the paper currently lacks scientific significance. This becomes especially clear when reading the introduction: 50 % of the introduction are a mere review of different techniques to observe wind speeds in the middle atmosphere. The only hint for the importance of wind observations is given in the beginning when the authors state that “together with temperature observations, they [wind observations] also offer more sophisticated studies of gravity waves”. Why is this not done in this paper? Showing different profiles of potential and kinetic energy densities does not qualify the paper as a “sophisticated study”. To put it short: the paper lacks a scientific question which is investigated and answered in the end. Without a clear scientific question the paper remains unacceptable. A mere publication of the wind and temperature observations is unjustified in my eyes, despite the fact that it is the currently most extensive data set.

   Following the suggestions of the short comment SC1 by *Dörnbrack* (2017) we included a quantification of the variability of winds and temperatures measured in the Arctic middle atmosphere; observations that have never be done before.

As mentioned earlier (e.g., *Meriwether and Gerrard*, 2004; *Drob et al.*, 2008; *Dörnbrack et al.*, 2017), wind observations in the middle atmosphere are of interest to infer direction and speed of gravity waves, to provide more input data and tests for empirical models like HWM07.

We highlighted this importance in the introduction.

2. Most of the very few conclusions drawn by the authors remain rather simple statements which purely describe the observations but the effects which lead to the observations remain in the dark. A few examples:

   P. 4, ll. 26–29: the conclusion that the northern hemispheric polar middle atmosphere is highly variable can certainly be considered as textbook knowledge and is therefore redundant.

   By quantifying the variability, as suggested by *Dörnbrack* (2017), we now added additional value to the observations and the comparison to model data.

   P. 5, ll. 21–29: the minor SSW and the following elevated stratopause event in 2012 have been well documented by previous studies. Also, as stated correctly by the authors, the mechanism for the formation of an elevated stratopause is known. Hence, I do not see the additional insights which are gained in this study from the combination of wind and temperature observations.

   We are sorry that the reviewer did not see the new insight, so we tried to clarify this in the manuscript. In summary, we clarify that these are the first direct observations of winds and temperatures during an elevated stratopause event in conjunction with the reformation of the polar vortex. As stated in the manuscript, this situation is not well represented in ECMWF data, highlighting the need for observations.

   We now highlighted in the manuscript why we think the data of this event is worth to be published: To quantify that a state-of-the-art weather model is still having some weaknesses in the middle atmosphere and even more observational data that are not assimilated in the model are needed to provide comparisons for model data.

   P. 8, l. 33 – p. 9, l. 2: The authors merely speculate on the effects which could cause the different gravity wave propagation conditions. Here, a thorough analysis is needed which investigates the propagation conditions in great detail.

   We believe that a detailed investigation of propagation conditions will distract from the main messages and is beyond the scope of this paper. We mention two possible explanations for the observed effect of varying gravity wave propagation: 1. multiple origins of gravity waves; 2. changing background conditions. While the second option is clearly visible in Fig. 5 (large temperature gradient and strong wind shear), the first option can not be excluded.

   We now mention in the manuscript that a clear distinction is not possible.

   P. 10, l. 9: Why is the Ekin/Epot ratio larger for the ECMWF data compared to the lidar data? What does this imply?

In general, a larger $E_{\mathrm{kin}}/E_{\mathrm{pot}}$ ratio indicates a larger ratio of wind fluctuations to temperature fluctuations. Inferring from the left panels of Fig. 8, the kinetic energy densities derived from lidar data and ECMWF data are of the same order, while potential energy densities are smaller in ECMWF data compared to lidar data. Hence, the day-to-day variability of temperatures is weaker in ECMWF than in the observations. This is obvious from the nightly mean profiles of January 2012 shown in Fig. 2.

We now mention this conclusion and the reference to Fig. 2 in the manuscript.

3. P. 8, ll. 25–26: the "approach using energy ratios has the advantage that an (energy weighted) intrinsic period for the ensemble of waves is calculated". This statement is wrong! *Geller and Gong* (2010) derive their formula from the polarization relations which are fulfilled only for one set of wave parameters (k, l, m, $\hat{\omega}$). If a superposition of waves is to be examined you have to take the sum over the squared wave perturbations in their equations 7) and 8). If you do so and insert the summed polarization relations, you will not end up with a formula, which you can solve for the average frequency. In fact *Geller and Gong* (2010) note in their appendix A1, that their approach always results in larger values of $\hat{\omega}$ than the mean value derived by the hodograph analysis.

   We have now revised this paragraph, clearly mentioning the assumptions made.

   N.B., *Geller and Gong* (2010) found smaller values of $\hat{\omega}$ with the energy ratio method than with the hodograph method, not larger.

   Furthermore, it should be noted that according to *Lane et al.* (2003) one can only see long-period inertial gravity waves in the horizontal wind speed fluctuations. Short period gravity waves exhibit more pronounced vertical wind perturbations. Thus the here applied methodology is already biased towards the large period gravity waves.

   This limitation of the method is now mentioned in the manuscript.

   If the authors want to infer gravity wave periods from their observations they have to use the hodograph approach instead of the energy approach. The energy approach can certainly be taken in the case of a quasi-monochromatic gravity wave field as shown by *Baumgarten et al.* (2015) but for an ensemble of waves it is not applicable.

   The hodograph method is only applicable to the case of one single gravity wave, not an ensemble of gravity waves (e.g., *Sato*, 1994). In the case of an ensemble of gravity waves it is hard or even impossible to identify the superposition of ellipses in the zonal and meridional wind fluctuations. Therefore the hodograph method cannot be applied to observations not showing a quasi-monochromatic gravity wave field. On the other hand, the energy ratio approach yields results when applied to observations showing a superposition of gravity waves. In this case it has to be noted, that the so derived $2\pi\hat{\omega}^{-1}$ is not the intrinsic period of a certain wave.

   We clearly address this issue in the manuscript now.

4. I still think that the comparison of the lidar measurements to the HWM07 model is not appropriate. HWM07 is a climatology and thus one cannot derive a meaningful mean profile from three years of observations in a highly variable surrounding (northern hemispheric polar middle atmosphere) which can be compared to this climatology. As a result the authors cannot differ whether the HWM07 takes too little observations into account (cf. p. 6, ll. 12–13) or whether their observations are simply too few for the comparison. Thus, I recommend removing the paragraph on the HWM07 comparison (p. 6, ll. 6–13) and instead focus the paper more on other aspects.

   We are aware of the limitations that the reviewer list and they have been clearly stated in the manuscript. However, we think that the comparison to HWM07 is valuable for the scientific community as highlighted by the references given in the manuscript.

5. It seems to me that the ECMWF model does not contain any gravity waves above 40–50 km altitude. Here a detailed investigation of the reasons for this behavior is needed. At the moment I do not see any physical reason why the gravity waves should not propagate to higher altitudes than 40–50 km.

   As mentioned by *Dörnbrack* (2017) “the numerical damping applied in the IFS” leads to an underestimation of the variability of winds and temperatures in the ECMWF data. We now mention in the manuscript that damping mechanisms in the ECMWF are the reason for the underestimation of variability, including a reference to *Jablonowski and Williamson* (2011).

   However, a “detailed investigation” of the behaviour of ECMWF regarding the damping of gravity waves is beyond the scope of this study and might be done by experts of the ECMWF model. This manuscripts provides strong hints that gravity waves are not well represented in the ECMWF model at altitudes above 40–50 km, including quantifications of this underestimation.

6. Regarding the methodology of extracting gravity waves from their observations: The authors state that they do not see any significant differences between their methodology and the Butterworth filter suggested by *Ehard et al.* (2015). If this is not the case, I wonder why the authors do not adopt the Butterworth filter? One of the reasons for using the Butterworth filter is that it ensures a comparability of different studies since the same part of the gravity wave spectrum is extracted from the observations. In fact, *Baumgarten et al.* (2017) recently showed that by applying different methods of gravity wave extraction, a different seasonal cycle of gravity wave activity can be derived.

   Numerous approaches to extract fluctuations caused by gravity waves have been applied to lidar data: filters in altitude (e.g., *Ehard et al.*, 2015), filters in time (e.g., *Rauthe et al.*, 2008), filters in both dimensions (e.g., *Baumgarten et al.*, 2015; *Zhao et al.*, 2017), or the variance method used by *Mzé et al.* (2014). Probably all of these methods have their advantages and drawbacks, and it is simply not possible to take all of them into account in every study about gravity waves. We mentioned the limitations of the approach we used in this study.

Concerning the comparability of different studies, the gravity wave spectrum taken into account depends not only on the applied vertical filtering technique but also on the temporal sampling of the data.

In a response to my previous review, the authors state that a further reason for not adopting the Butterworth filter is that “When applied to ECMWF data, the Butterworth and the spline method yielded physically dubious results (see Fig. 2): E.g., altitude profiles of GWED derived with the Butterworth method always showed similar oscillating behaviour above ≈ 65 km altitude; the ratio Ekin=Epot showed values < 1 for the spline and the Butterworth method, which can’t be true for gravity waves.” This argument can be dismissed in line of my major comment 5), since if there are no gravity waves in the ECMWF model above 40–50 km altitude, the results obtained by all methods are unphysical.

Given that it cannot be ruled out that ECMWF data might contain some gravity waves above 40–50 km altitude, the approach applied in this study was the only one of the three approaches tested that allowed to quantify the underestimation of GWED in ECMWF data.

Furthermore, the 10 h averaging applied by the authors has a significant disadvantage when it comes to analyzing the ECMWF data. I guess (see minor comments) that the authors use data from a different ECMWF run after 00 UTC. The corresponding switch from one ECMWF run to another is very likely to introduce a sudden jump of the temperature profile, which will be detected by the authors method, but not by a vertical Butterworth filter. For example the larger Ekin/Epot ratios by the ECMWF compared to the lidar observations (p. 10, l. 9) could easily be an effect of the different ECMWF runs and analysis used here. In fact I think what you see in the large scale wave energy density is mostly affected by the data assimilation of the ECMWF and not the model dynamics. This has to be investigated with great care!

As the large-scale energy density relies on nightly mean profiles, we do not think that by using data of two different ECMWF runs per night the results might be corrupted.

Minor comments

1. In line with major comment 6): I do not know at which times the authors use analysis data and at which times they use forecast data. For example, ECMWF analysis data is available at 00, 06, 12 and 18 UTC, but one can also retrieve forecast data for these times. Also the authors do not state from which runs the data are taken (i.e. runs initialized at 00 or 12 UTC, or a combination of both). This has to be clarified.

   As already stated in the manuscript, we use forecast data with 1 h time resolution.

We have clarified in the manuscript that we use both runs: the 00 UTC run for data between midnight and noon and the 12 UTC run for data between noon and midnight.

Furthermore, I was wondering, whether you extract the lidar data really at the named position, or whether you interpolate it horizontally to your lidar position?

We extracted the ECMWF data with horizontal resolution of 0.25° and interpolated these data on pressure levels horizontally to the location of ALOMAR.

This is now clarified in the manuscript.

2. Regarding the measurement uncertainties: At which altitudes do the maximum uncertainties usually appear? How do you treat measurement profiles for which the uncertainties appear at lower altitudes, e.g. 60 km? Do you have further constraints to insure the quality of your observations?

   The measurement uncertainties increase with altitude, as the amount of received backscattered laser photons decrease with altitude. Hence, highest uncertainties appear generally at the highest altitudes. Profiles reach only as high as the measurement uncertainty is below the thresholds mentioned in Sect. 3. Raw signal profiles (5 min integration) which are obviously disturbed by poor signal quality (e.g., due to clouds) are discarded prior to the 1 h integration and subsequent temperature and wind retrieval. As only very few profiles were affected, we did not add this technical aspect in the revised manuscript.

   We expanded the respective paragraph in the manuscript.

3. P. 5, ll. 12.–13: You state the “also” (why also? what else varies?) small vertical variability of the wind profiles and in the next sentence you state “very pronounced gravity wave structures”. Aren’t both statements contradictory?

   We agree that the phrasing was misleading and clarified it.

4. P. 5, l. 35: “comparison of lidar data with ECMWF (. . .) for the whole data set”: since you compare two different ECMWF cycles to your observations it is misleading to average both cycles like done in Fig. 4d). In fact it seems to me that by averaging both cycles the deviations between the ECMWF and the observations decrease.

   Since there is no Fig. 4(d) we assume the reviewer is referring to Fig. 3(d). We like to point out that Fig.s 3(a)–(c) and Fig.s 4(a) and (b) clearly show the results separated for the different model cycles. Since this might have gone undetected we have now added the information about the model cycles in the respective figures captions.

   Also on p. 6, l. 19, I am not astonished that the comparison is nonuniform throughout the years, since you compare different cycles to your observations. This has to be evaluated in more detail and with more care!

We have carefully separated the data set according to different model cycles and now highlighted this information in the captions of Fig.s 3 and 4.

It is beyond the scope of this manuscript to investigate differences between ECMWF cycles and why ECMWF data might match differently to certain atmospheric conditions.

Also later in ll. 23–26, you should state the cycles used by the other studies.

Le Pichon et al. (2015) use ECMWF IFS cycles 38r1 and 38r2; see their Sect. 2.3 for details. *Rüfenacht et al.* (2014) use "ECMWF operational analysis data" of various cycles (*Rüfenacht et al.*, 2016): "36r2 (September to November 2010), 36r4 (November 2010 to May 2011), 37r2 (May to November 2011), 37r3 (November 2011 to June 2012), 38r1 (June 2012 to June 2013), 38r2 (June to November 2013) and 40r1 (November 2013 to February 2015)".

We now note in the manuscript that other studies use different IFS cycles.

5. P. 7, l. 4: what is the RMS, I guess the authors mean "root mean square" but of what? Please clarify and also explain the abbreviation. Maybe also give a short explanation as to why an increase of the RMS is "expected for the effect of gravity waves".

   We now included in the manuscript the abbreviation (root mean square) and clarified that we mean the root mean square of the fluctuations as an indicator of gravity wave activity. We also added the explanation of the expected behaviour.

6. Figure 4b) is unnecessary and should be removed. The information on the deviation of the different profiles from one another is already contained in the profiles and the according standard deviations (shaded area) in Figure 4a).

   We have considered removing this panel, but since the shape of the distribution cannot be inferred from Fig. 4(a) we decided to keep this panel.

7. In my eyes also Figure 5 is unnecessary, since the information on gravity wave activity is already contained in Figure 6 and the paragraph (p. 6, l. 30 – p. 7, ll. 2) does not give substantial new information. Furthermore, the conclusions drawn in this paragraph again remain pure speculation.

   This figure is the only example showing the actual 1 h profiles of lidar and ECMWF data. Furthermore, the discussions of Fig. 4(c) and Fig. 6 build on this figure.

8. A general comment regarding the Figures: most axis are rather small and difficult to read. E.g. values of the RMS profiles in Figure 5 cannot be inferred. Furthermore, all plots showing Epot and Ekin on a log axis would definitely benefit from a larger aspect ratio so that concrete values can be inferred by the readers more easily. Furthermore, it should be avoided that plotted values are smaller than the axis values (1st panel, Fig. 3c; 3rd panel, Fig. 8a).

   We increased the font size of the tick labels and axis labels. As the RMS profiles in Fig. 5 are intended to have quality character only, to qualitatively compare fluctuations and measurement uncertainties, we see no need to enlarge this figure. Concerning clipped profiles in Fig. 3(c) and Fig. 8(a), we used the same axis scaling for the sake of comparison of various figures.

Technical corrections

1. P. 1, l. 4 and throughout the text: "month-mean" should read "monthly mean", the same for "night-mean".

   done

2. P. 2, l. 8: "then" should read "than"

   done

3. P. 2, l. 9: give the names for the models (ECMWF, HWM07) at the first appearance of the abbreviations in the text

   done

4. P. 3, ll. 17–19: it might be of help for the reader to slightly change the order of the sentences: "To retrieve winds (...) The temperature retrieval relies (...) The two individually derived temperature profiles (...)" Also cite *Hauchecorne and Chanin* (1980) for the retrieval of your temperature profile.

   done

5. P. 4, l. 11: the vertical resolution of the two ECMWF model cycles should be stated.

   The altitude profiles of the ECMWF data already contained small ticks to mark the respective model levels; indicating that the vertical resolution decreases with altitude.

   We now included in the manuscript that cycle Cy37r3 has 91 model levels and Cy40r1 has 137 model levels.

6. P. 4, l. 12: what is the vertical resolution of the lidar data? On p. 3, l. 27 you state that the lidar data is smoothed with a "window size of 3 km" is this the vertical resolution of the lidar data? Your profiles look way smoother than just one point every 3 km.

   The internal range resolution of the lidar instrument is 50 m; the data were gridded to a raster of 150 m vertical resolution. These data were then smoothed with a running box filter with window size of 3 km.

   We clarified this in Sect. 3.

7. P. 4, l. 32: "or even split, *and* warmer air"

   done by using a semicolon instead of a comma

8. P. 5, l. 9: “Only *a* few days later”

   done

9. P. 5, ll. 10 & 11: “some 20 K colder/warmer” – colloquial, state precise values

   done

10. P. 5, ll. 11 & 12: “weak east/west/southward” should read “weakly east/west/southward”

    done

11. P. 6, l. 16: “way too low” – colloquial, state precise values

    done

12. P. 6, l. 20: “it is good below 60 km altitude”, please quantify. “Good” can mean anything.

    done

13. P. 6, l. 26: “some deviations in the mesosphere”, please quantify.

    done

References

Baumgarten, G., J. Fiedler, J. Hildebrand, and F.-J. Lübken, Inertia gravity wave in the stratosphere and mesosphere observed by doppler wind and temperature lidar, *Geophys. Res. Lett.*, *42*(24), 10,929–10,936, doi:10.1002/2015GL066991, 2015GL066991, 2015.

Baumgarten, K., M. Gerding, and F.-J. Lübken, Seasonal variation of gravity wave parameters using different filter methods with daylight lidar measurements at midlatitudes, *J. Geophys. Res.*, accepted, 2017.

Dörnbrack, A., S. Gisinger, and B. Kaifler, On the interpretation of gravity wave measurements by ground-based lidars, *Atmosphere*, *8*(3), doi:10.3390/atmos8030049, 2017.

Dörnbrack, A., Interactive comment on “Winds and temperatures of the Arctic middle atmosphere during January measured by Doppler lidar” by Jens Hildebrand et al., doi:10.5194/acp-2017-167-SC1, 2017.

Drob, D. P., J. T. Emmert, G. Crowley, J. M. Picone, G. G. Shepherd, W. Skinner, P. Hays, R. J. Niciejewski, M. Larsen, C.-Y. She, J. W. Meriwether, G. Hernandez, M. J. Jarvis, D. P. Sipler, C. A. Tepley, M. S. O’Brien, J. R. Bowman, Q. Wu, Y. Murayama, S. Kawamura, I. M. Reid, and R. A. Vincent, An empirical model of the Earth’s horizontal wind fields: HWM07, *J. Geophys. Res.*, 2008.

Ehard, B., B. Kaifler, N. Kaifler, and M. Rapp, Evaluation of methods for gravity wave extraction from middle-atmospheric lidar temperature measurements, *Atmos. Meas. Tech.*, *8*(11), 4645–4655, doi:10.5194/amt-8-4645-2015, 2015.

Geller, M. A., and J. Gong, Gravity wave kinetic, potential, and vertical fluctuation energies as indicators of different frequency gravity waves, *J. Geophys. Res.*, *115*(D11), n/a–n/a, doi:10.1029/2009JD012266, 2010.

Hauchecorne, A., and M.-L. Chanin, Density and temperature profiles obtained by lidar between 35 and 70 km, *Geophys. Res. Lett.*, *7*, 565–568, doi:10.1029/GL007i008p00565, 1980.

Jablonowski, C., and D. L. Williamson, *The Pros and Cons of Diffusion, Filters and Fixers in Atmospheric General Circulation Models*, pp. 381–493, Springer Berlin Heidelberg, Berlin, Heidelberg, doi:10.1007/978-3-642-11640-7_13, 2011.

Lane, T. P., M. J. Reeder, and F. M. Guest, Convectively generated gravity waves observed from radiosonde data taken during mctex, *QJRMS*, *129*(590), 1731–1740, doi:10.1256/qj.02.196, 2003.

Le Pichon, A., J. D. Assink, P. Heinrich, E. Blanc, A. Charlton-Perez, C. F. Lee, P. Keckhut, A. Hauchecorne, R. Rüfenacht, N. Kämpfer, D. P. Drob, P. S. M. Smets, L. G. Evers, L. Ceranna, C. Pilger, O. Ross, and C. Claud, Comparison of co-located independent ground-based middle atmospheric wind and temperature measurements with numerical weather prediction models, *J. Geophys. Res.*, *120*(16), 8318–8331, doi:10.1002/2015JD023273, 2015JD023273, 2015.

Meriwether, J. W., and A. J. Gerrard, Mesosphere inversion layers and stratosphere temperature enhancements, *Rev. Geophys.*, *42*(3), RG3003, doi:10.1029/2003RG000133, 2004.

Mzé, N., A. Hauchecorne, P. Keckhut, and M. Thétis, Vertical distribution of gravity wave potential energy from long-term rayleigh lidar data at a northern middle-latitude site, *J. Geophys. Res.*, *119*(21), 12,069–12,083, doi:10.1002/2014JD022035, 2014JD022035, 2014.

Rauthe, M., M. Gerding, and F.-J. Lübken, Seasonal changes in gravity wave activity measured by Lidars at mid-latitudes, *Atmos. Chem. Phys.*, *8*, 6775–6787, 2008.

Rüfenacht, R., A. Murk, N. Kämpfer, P. Eriksson, and S. A. Buehler, Middle-atmospheric zonal and meridional wind profiles from polar, tropical and midlatitudes with the ground-based microwave doppler wind radiometer wira, *Atmos. Meas. Tech.*, *7*(12), 4491–4505, doi:10.5194/amt-7-4491-2014, 2014.

Rüfenacht, R., K. Hocke, and N. Kämpfer, First continuous ground-based observations of long period oscillations in the vertically resolved wind field of the stratosphere and mesosphere, *Atmos. Chem. Phys.*, *16*(8), 4915–4925, doi:10.5194/acp-16-4915-2016, 2016.

Sato, K., A statistical study of the structure, saturation and sources of inertio-gravity waves in the lower stratosphere observed with the mu radar, *J. Atmos. Terr. Phys.*, 1994.

Zhao, J., X. Chu, C. Chen, X. Lu, W. Fong, Z. Yu, R. M. Jones, B. R. Roberts, and A. Dörnbrack, Lidar observations of stratospheric gravity waves from 2011 to 2015 at McMurdo (77.84° S, 166.69° E), Antarctica: Part I. Vertical wavelengths, periods, and frequency and vertical wavenumber spectra, *J. Geophys. Res.*, pp. n/a–n/a, doi: 10.1002/2016JD026368, 2016JD026368, 2017.

Reply to acp-2017-167-RC2, a review of the manuscript ACP-2017-167 “Winds and temperatures of the Arctic middle atmosphere during January measured by Doppler lidar”

Jens Hildebrand et al.

June 26, 2017

The paper presents wind and temperature measurements by lidar technique at the arctic location of Andoya (69° N). The data are from three Januarys in 2012, 2014 and 2015. The measured night time profiles extend form approx. 30km to 85 km altitude with a temporal resolution of 1 hour. Profiles are compared with corresponding ones from ECMWF and HWM07. Significant differences in temperature and wind between the models and the measurements are reported. In a second part of the paper the authors deduce potential and kinetic gravity wave energy densities based on the measured temporal fluctuations of temperatures and winds.

The paper is carefully and clearly written and easy to follow. Figures are clear and document well the results.

It has to be noted, and the authors clearly summarize this in the introduction, that measured wind profiles are very rare and accordingly very few papers present measured data. Further, the number of publications showing datasets over some extended periods are even more scarce. This paper presents extended data for three Januarys and therefore significantly contributes to an area of middle atmospheric research where the data amount is small so far. This is particularly important as in recent years experimental techniques suffer from declining interest and more weight is put on modeling. Data with high quality as presented in this paper are therefore of extreme value for the validation and improvement of models and they merit to be published. This is particularly true for the data discussed in the current paper.

I therefore recommend to publish the paper with some minor modifications or corrections.

Comments

1. In the section about data, page 3, lines 28 etc. it is not clear how the measurement uncertainties are defined. On the one hand they say that typical values are 0.5K and 3m/s for temperature and wind resp. However then it is said that data with uncertainty values roughly ten times higher are also considered. Please clarify why

this large range of uncertainties exists and why you take all these data with high uncertainty into consideration.

Measurement uncertainties arise from the statistics of the backscattered laser photons detected. As less photons are recorded for higher altitudes (as there are less air molecules), the measurement uncertainty increases with altitude. Therefore, values with a certain range of measurement uncertainties have to be taken into account. As can be seen in Fig. 5 the thresholds mentioned in Sect. 3 are exceeded for 1 h profiles at ≈ 88 km and ≈ 78 km altitude for temperatures and winds, respectively, while nightly mean profiles exceed the thresholds at higher altitudes (since more data are taken into account).

We expanded the respective paragraph in the manuscript.

2. Section 4 about results shows high variability in temperature and wind from night to night. The January variability particularly in wind significantly depends on where the measurement is taken with respect to the vortex edge. Indeed the authors several times say that the position of the vortex is important but they do never show where it actually is. Unfortunately it is not possible to find out when the measurement was inside or outside of the vortex. I strongly recommend that the authors separate the data set in two, one with profiles from inside and the other one from outside the vortex. Also the comparison with the models might then change. The large differences between model and data might be explained by such an inappropriate comparison. Section 4.2 as well is linked to the polar vortex and the authors say that a reformation of the vortex took place. Unfortunately again it is not clear how the situation was at Andoya where the observations took place. Please expand this section regarding the vortex.

   To get information about the position of the polar vortex relative to ALOMAR, we examine the potential vorticity at a given potential temperature level, as suggested by *Rex et al.* (1998) and applied by, e.g., *Grooß and Müller* (2003): The edge of the polar vortex is defined as potential vorticity of 36 PVU at the 475 K potential temperature (Θ) level. Using ECMWF data we derive the potential vorticity at $\Theta = 475$ K for each 1 h profile of each night (linear interpolation of potential vorticity from model/pressure levels to Θ levels). A night is then considered as "inside" or "outside" of the polar vortex, if all (or all but one) 1 h profiles have potential vorticity smaller or larger 36 PVU, respectively; during nights with multiple "inside" and "outside" profiles the vortex edge lies above the site. It has to be noted that the polar vortex might bend and twist and therefore the vortex location as defined at 475 K (≈ 19 km altitude) may not always represent the situation in the upper strato- and mesosphere.

   Figure 1 shows the same data as Fig. 3 of the manuscript but split depending on relative vortex positions. In the cumulated data (panel d) temperatures are higher inside the vortex than outside, according to expectation. This behaviour is not seen in January 2012 with lower "inside" than "outside" temperatures below 50 km altitude and January 2014 with only very small differences between "inside" and "outside" temperatures. Note that the "vortex edge" profiles are not intermediate profiles between the "inside" and "outside" profiles. Hence, the temporal development of the dynamics (as discussed in Sect. 4.2 for January 2012) seem to surface more dominant than the – somewhat static – distinction between being inside or outside the polar vortex; furthermore, each data subset consists of few nights only. Therefore, and because the lidar-to-ECMWF comparison seems not to differ fundamentally for the separated data sets, we don't discuss all the aspects mentioned in the manuscript for the separated data.

Nevertheless, we expanded Sect. 4.2 about the SSW in January 2012 and mention for each profile in Fig. 2 of the manuscript to which class ("inside", "outside", "vortex edge") it belongs.

Technical corrections

1. Abstract line 16: The sentence "The total LWED." does not make sense. Something is lost here . page 3, line 25: . . . was acquired during the nights in January 2012. . .

   done; done

2. page 6, line 12: either use "this discrepancy" or "these discrepancies"

   done

References

Grooß, J.-U., and R. Müller, The impact of mid-latitude intrusions into the polar vortex on ozone loss estimates, *Atmos. Chem. Phys.*, *3*(2), 395–402, doi:10.5194/acp-3-395-2003, 2003.

Rex, M., P. von der Gathen, N. R. P. Harris, D. Lucic, B. M. Knudsen, G. O. Braathen, S. J. Reid, H. De Backer, H. Claude, R. Fabian, H. Fast, M. Gil, E. Kyrö, I. S. Mikkelsen, M. Rummukainen, H. G. Smit, J. Stähelin, C. Varotsos, and I. Zaitcev, In situ measurements of stratospheric ozone depletion rates in the arctic winter 1991/1992: A lagrangian approach, *J. Geophys. Res.*, *103*(D5), 5843–5853, doi: 10.1029/97JD03127, 1998.

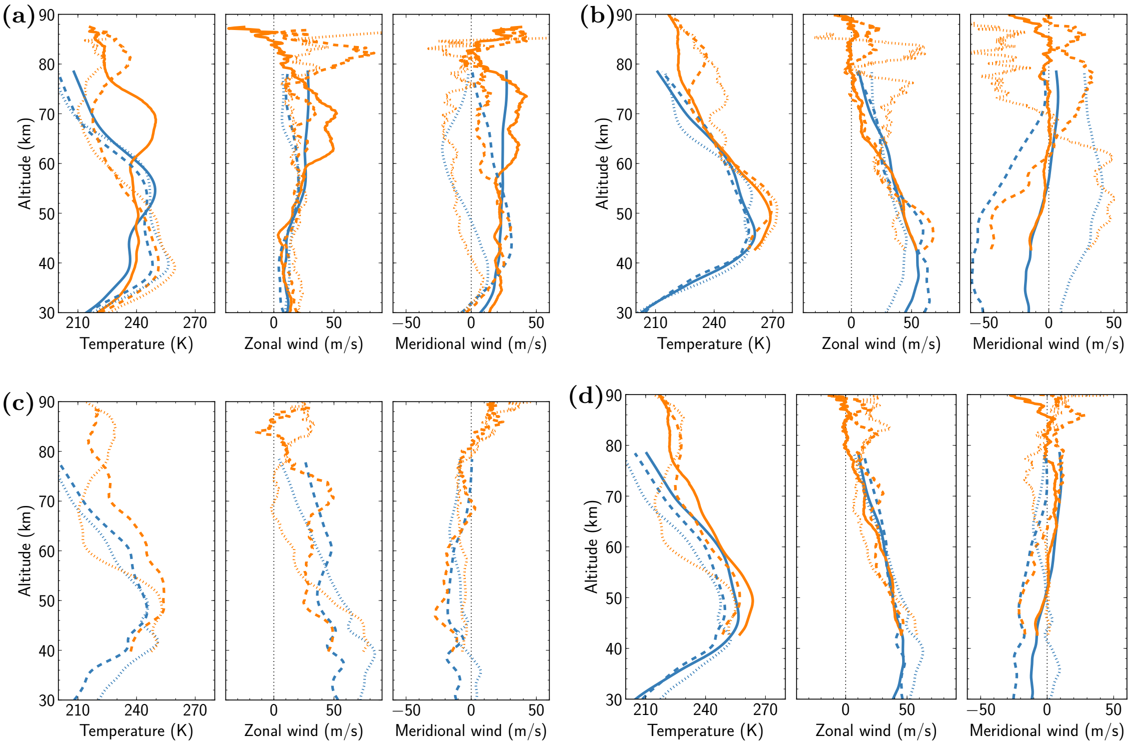

Figure 1 Like Fig. 3 of the manuscript, but data set split depending on relative vortex positions. January mean temperatures and horizontal winds for the years 2012 (a), 2014 (b), and 2015 (c), and cumulated data (d). Orange: ALOMAR RMR lidar, blue: ECMWF. Solid lines: inside the polar vortex, dashed lines: outside the polar vortex, dotted lines: vortex edge.

Reply to acp-2017-167-SC1, an interactive comment on the manuscript ACP-2017-167 “Winds and temperatures of the Arctic middle atmosphere during January measured by Doppler lidar”

Jens Hildebrand et al.

June 26, 2017

Reading the paper and the comment by the reviewer I get the impression that the achievement to observe both wind and temperature fields in the middle atmosphere is largely underestimated by the reviewer. For me, the scientific significance of the paper is at least threefold:

1. the clear and detailed documentation of the simultaneous wind and temperature measurements and a QUANTIFICATION of the variability in wind and temperature over a LARGE height region; even if the conclusion the Arctic winter stratosphere/mesosphere is highly variable is “text book” knowledge, the ultimate quantification can turn this statement into a scientifically significant conclusion

   We now included a discussion of the variability of temperatures and winds within single months, including a quantification for different altitudes.

2. the comparison with model profiles which shows a great agreement up to about 45 km altitude (if I would be the author, I would mention this astonishing agreement much more) – just to make it clear: the authors compare INDEPENDENT data, the lidar profiles were not assimilated into the IFS; above this altitude, the numerical damping applied in the IFS is certainly underestimating the variability found in the observations – this could be a little bit more explained; but again it is the quantification of the agreement and disagreement which make the results scientifically relevant

   We now highlighted the good agreement of winds in lidar data and ECMWF data and improved the inter-comparison of both data sets with additional quantification. And we included a short explanation of the damping of gravity waves in the ECMWF model data, including a reference to a detailed overview of various damping approaches used in atmospheric modelling (*Jablonowski and Williamson*, 2011).

3. the exemplary derivation anf presentation that wind observation are a MUST in order to derive intrinsic wave properties; the recent papers by *Zhao et al.* (2017)

and by *Dörnbrack et al.* (2017) point exactly in this direction and I think the present paper is an excellent contribution to push the need for such observations forward

We now highlighted the importance of wind observations in the introduction by including additional references.

Hope to see this work publsihed soon!

References

Dörnbrack, A., S. Gisinger, and B. Kaifler, On the interpretation of gravity wave measurements by ground-based lidars, *Atmosphere*, *8*(3), doi:10.3390/atmos8030049, 2017.

Jablonowski, C., and D. L. Williamson, *The Pros and Cons of Diffusion, Filters and Fixers in Atmospheric General Circulation Models*, pp. 381–493, Springer Berlin Heidelberg, Berlin, Heidelberg, doi:10.1007/978-3-642-11640-7_13, 2011.

Zhao, J., X. Chu, C. Chen, X. Lu, W. Fong, Z. Yu, R. M. Jones, B. R. Roberts, and A. Dörnbrack, Lidar observations of stratospheric gravity waves from 2011 to 2015 at McMurdo (77.84° S, 166.69° E), Antarctica: Part I. Vertical wavelengths, periods, and frequency and vertical wavenumber spectra, *J. Geophys. Res.*, pp. n/a–n/a, doi:10.1002/2016JD026368, 2016JD026368, 2017.

Winds and temperatures of the Arctic middle atmosphere during January measured by Doppler lidar

Jens Hildebrand[1], Gerd Baumgarten[1], Jens Fiedler[1], and Franz-Josef Lübken[1]

[1]Leibniz-Institute of Atmospheric Physics at the Rostock University, Kühlungsborn, Germany

Correspondence to: J. Hildebrand (hildebrand@iap-kborn.de)

Abstract. We present an extensive data set of simultaneous temperature and wind measurements in the Arctic middle atmosphere. It consists of more than 300 h of Doppler Rayleigh lidar observations obtained during three January seasons 2012, 2014, and 2015, and covers the altitude range from 30 km up to about 85 km. The data set reveals large year-to-year variations of ~~month-mean~~ monthly mean temperatures and winds, which in 2012 are caused by a sudden stratospheric warming. The temporal evolution of winds and temperatures after that warming are studied over a period of two weeks, showing an elevated stratopause and the reformation of the polar vortex. The ~~month-mean~~ monthly mean temperatures and winds are compared to data extracted from the Integrated Forecast System of the European Centre for Medium-Range Weather ~~Forecast~~Forecasts (ECMWF) and the Horizontal Wind Model (HWM07). ~~We~~ Lidar and ECMWF data show excellent agreement of mean zonal and meridional winds below ≈ 55 km altitude, but we also find mean temperature, zonal wind, and meridional wind differences of up to 20 K, 20 m s^{-1}, and 5 m s^{-1}, respectively, ~~between lidar observations and ECMWF data and~~ and of up to 30 m s^{-1} between lidar observations and HWM07 data. From the fluctuations of temperatures and winds within single nights we extract the potential and kinetic gravity wave energy density (GWED) per unit mass. It shows that the kinetic GWED is typically 5 to 10 times larger than the potential GWED, the total GWED increases with altitude with a scale height of ≈ 16 km. Since temporal fluctuations of winds and temperatures are underestimated in ECMWF, the total GWED is underestimated as well by a factor of 3 to 10 above 50 km altitude. Similarly, we estimate the energy density per unit mass for large-scale waves (LWED) from the fluctuations of ~~night-mean~~ nightly mean temperatures and winds. The total LWED is roughly constant with altitude. The ratio of kinetic to potential LWED varies with altitude over two orders of magnitude. LWEDs from ~~ECWMF~~ ECMWF data show similar results as the lidar data. From the comparison of GWED and LWED follows that large-scale waves carry about 2 to ~~6~~ 5 times more energy than gravity waves.

1 Introduction

Winds in the middle atmosphere play an important role for atmospheric dynamics; e.g., filtering of gravity waves is controlled by the background wind field (e.g., Lindzen, 1981; Gill, 1982; Nappo, 2002). As these gravity waves transport energy and momentum over long distances, winds indirectly affect large-scale circulations (e.g., Geller, 1983; Holton, 1983). Therefore, wind measurements in the middle atmosphere with reasonable temporal and vertical resolution are of special interest ~~(Meriwether and Gerrard, 2004)~~(Meriwether and Gerrard, 2004; Drob et al., 2008). But not only do wind measurements provide additional information about atmospheric stability, together with temperature observations they also offer more sophisticated studies of gravity waves (e.g., Eckermann et al., 1995; Zink and Vincent, 2001; Placke et al., 2013; Bossert et al., 2014; Baumgarten et al., 2015) ~~then~~ than studying gravity waves solely from temperature measurements (e.g., Chanin and Hauchecorne, 1981; Whiteway and Carswell, 1995; Alexander et al., 2011). In a recent study, Dörnbrack et al. (2017) point out that information about background wind is essential to correctly interpret ground-based gravity wave observations regarding identified phase lines and the vertical propagation direction. However, simultaneous wind and temperature measurements covering a wider altitude range of the middle atmosphere are rare (e.g., Goldberg et al., 2004). The main reason is the technical challenge of wind measurements in these altitudes. Radars do not cover the altitude range between 20 and 60 km due to the absence of free electrons. Balloons reach only top altitudes of 30–40 km. Meteorological rockets, equipped with chaff, falling spheres or starutes, are able to measure winds in the entire middle atmosphere between about 20 and 100 km (e.g., Widdel, 1987, 1990; Schmidlin et al., 1991; Lübken and Müllemann, 2003; Müllemann and Lübken, 2005). Such rocket soundings yield a reasonable vertical resolution, but are conducted only sporadically. Data from several campaigns at Arctic sites, which cover longer periods, have been published by, e.g., Meyer et al. (1987), Lübken and Müllemann (2003), and Müllemann and Lübken (2005). Microwave radiation is used to measure the Doppler shift of thermally excited molecules. This technique is used, e.g., by MLS onboard the Aura satellite (Wu et al., 2008) and the ground-based WIRA instrument (Rüfenacht et al., 2012, 2014), and had been used by the SMILES instrument onboard the ISS (Baron et al., 2013). Another approach is to measure the Doppler shift of airglow lines. This was done by the instruments HRDI and WINDII onboard UARS (Hays et al., 1993; Shepherd et al., 1993); TIDI onboard the TIMED satellite (Killeen et al., 2006) still employs this technique. A ground-based instrument which measures wind speeds by analyzing airglow is ERWIN II (Kristoffersen et al., 2013); since it relies on three dedicated airglow emissions only, its height range is limited to layers between 87 and 97 km altitude. An indirect approach to estimate wind speeds from satellite observations is to retrieve geostrophic winds from geopotential heights on fixed pressure levels (e.g., Randel, 1987). The lidar technique allows to derive wind speeds directly from measuring the Doppler shift of light backscattered at moving particles. Resolving the Doppler shift is technically challenging and wind lidars are therefore sophisticated instruments. While sodium resonance lidars yield wind speeds in the sodium layer between about 80 km and 105 km altitude (e.g., Liu et al., 2002; She et al., 2002; Franke et al., 2005; Yuan et al., 2012), Rayleigh lidars cover mainly altitudes below 50 km (e.g., Tepley, 1994; Friedman et al., 1997; Souprayen et al., 1999; Huang et al., 2009; Xia et al., 2012). Reports about regular wind measurements by lidar are scarce: Tepley (1994) presents winds between 10 and 60 km altitude, derived during 43 nights at the tropical site Arecibo; Souprayen et al. (1999) derived horizontal winds during 170 nights in the altitude range 8–50 km at mid latitudes; regular observations of horizontal winds with sodium resonance lidars (80–105 km) were presented by Franke et al. (2005) and Yuan et al. (2012) for tropical and mid latitudes, respectively.

The ALOMAR Rayleigh/Mie/Raman (RMR) lidar is the only instrument that derives both horizontal wind components and temperature simultaneously from the upper stratosphere up to the mesosphere. In this study, we present horizontal winds and temperatures obtained by DoRIS, the Doppler Rayleigh Iodine Spectrometer of the ALOMAR RMR lidar, during the three January seasons 2012, 2014, and 2015, in total more than 300 h of observations. They provide the most extensive data set of simultaneous wind and temperature measurements in the middle atmosphere, and allow us to study the variability of temperatures and winds regarding year-to-year variations, the temporal evolution on time scales of days, e.g., after the stratospheric warming in January 2012, and during single nights. This study also analyzes the representation of temperatures and winds by the ~~ECWMF~~ Integrated Forecast System~~and the model~~ (IFS) of the European Centre for Medium-Range Weather Forecasts (ECMWF) and the Horizontal Wind Model (HWM07) regarding the comparison to observational data. Subsequently, potential and kinetic energy densities of gravity waves and large-scale waves are calculated and analyzed.

2 Instrument

The ALOMAR RMR lidar (69.3°N, 16.0°E) is a twin lidar with two identical transmitting lasers, two identical receiving telescopes and one detection system. It measures temperatures and aerosols in the middle atmosphere on routine basis since 1997 (von Zahn et al., 2000; Schöch et al., 2008). Since 2009 the lidar measures wind speeds as well, using the Doppler Rayleigh Iodine Spectrometer DoRIS (Baumgarten, 2010). Detailed descriptions of the instrumental setup and the wind retrieval as well as initial results for the altitude range 30–85 km were presented by Baumgarten (2010), Hildebrand et al. (2012), and Lübken et al. (2016). Basically, the ~~temperature~~ wind retrieval relies on ~~hydrostatic integration of altitude profiles of relative air density. To retrieve winds,~~ measuring the Doppler shift of the backscattered light ~~is measured~~ using iodine absorption spectroscopy; temperatures are retrieved by hydrostatic integration of altitude profiles of relative air density (Kent and Wright, 1970; Hauchecorne and Chanin, 1980). The two individually derived temperature profiles for both lasers/telescopes are averaged to one temperature profile; this reduces the measurement uncertainty, but the amplitudes of gravity waves are not affected significantly (since the distance of both sounding volumes is much shorter than typical horizontal wavelengths of the inertia gravity waves which are most prominent in the 1 h averaged profiles: 40 km distance at 80 km altitude compared to wavelengths of several hundred kilometers (e.g., Baumgarten et al., 2015)).

3 Data

The data set used for this study was acquired during nights in January 2012, 2014, and 2015. January 2013 is excluded since there exist only about 10 h of nighttime horizontal wind observations. The data ~~was~~ were integrated over 1 h~~and smoothed in altitude~~. The vertical resolution is 150 m, but data were smoothed with a ~~window~~ running window with a size of 3 km. Typical uncertainties are 0.5 K and $3\,\mathrm{m\,s^{-1}}$ at 50 km altitude but increase with altitude (due to less received backscattered light from higher altitudes, mainly due to decreasing air density). The retrieved temperature and wind speed profiles considered in this study are limited to measurement uncertainties of $\Delta T \leq 5\,\mathrm{K}$ and $\Delta u = \Delta v \leq 20\,\mathrm{m\,s^{-1}}$, respectively. Due to technical issues the lower altitude limit in January 2014 and January 2015 is about 40 km instead of 30 km. As lidar operations depend on weather conditions, the observations are unequally distributed over the years: 65 h during seven nights between 19 and 30 January 2012, 170 h during 16 nights between 10 and 31 January 2014, and 78 h during five nights between 19 and 24 January 2015. Table 1 lists the nights and the respective duration of the lidar observations. Note ~~,~~that although the sampling is quite sparse in January 2012 and 2015, these are the only available simultaneous wind and temperature observations in the Arctic stratosphere and mesosphere. For the analysis of wave phenomena in Sect. 4.4 we restrict the data set to nights with observations of at least 10 h; this reduces the number of observations taken into account to two thirds of the entire data set, but the fraction of data taken into account is reduced by only one tenth. Table 2 gives an overview of the observations taken into account for analyses based on all ~~the nights and the~~ nights and long observations only.

Additionally, model data are used for the location of ALOMAR: The European Centre for Medium-Range Weather Forecasts ~~(ECMWF)~~ provides the Integrated Forecast System IFS. We extracted data with horizontal resolution T1279 at the location 69.28° N, 16.01° E~~. As available by~~ (the data are available with horizontal resolution of 0.25°, we interpolated these horizontally on pressure levels to our location). We use data from the forecast system ~~, the temporal resolution is~~ with a temporal resolution of 1 h; hence, lidar data and ECMWF data have the same temporal sampling. Profiles between midnight and noon were taken from the model run initialized at 00 UTC, profiles between noon and midnight were taken from the 12 UTC run. For January 2012 we used cycle ~~Cy36r1~~Cy37r3, and for January 2014 and 2015 we used cycle ~~Cy38r2~~Cy40r1. Both cycles differ, amongst others, in their vertical resolution, especially at higher altitudes: Cy37r3 has 91 model levels, Cy40r1 has 137 model levels. For each single 1 h profile the pressure coordinate is converted into geometric altitude; the profile is then interpolated to the vertical resolution of the lidar data. The Horizontal Wind Model HWM07 is an empirical model that accumulates data from different instruments obtained over fifty years (Drob et al., 2008). Therefore, the model does not contain any year-to-year variation, but has more character of a climatology. We extracted data on an hourly basis (corresponding to the temporal sampling of the lidar) for the location 69.3° N, 16.0° E.

4 Results

4.1 January variability

For a first descriptive presentation of the data set, Fig. 1 shows mean altitude profiles of temperatures and horizontal winds for Januaries 2012, 2014, and 2015. It is evident that the mean profiles for the three years differ remarkably. While in 2012 highest temperatures of 245 K occur at 38 km altitude, highest temperatures in 2014 are 270 K and occur at 50 km altitude; the temperatures in 2012 and 2015 show enhanced variability around 70 and 60 km altitude, respectively, but there is no such enhanced variability in 2014. The strength of the eastward zonal winds varies, too: In 2014 and 2015 highest wind speeds of 50–70 $\mathrm{m\,s^{-1}}$ occur around 45 km altitude, while zonal wind in 2012 is weak at this height; but in 2012 highest zonal wind speeds occur between 62 and 72 km, with enhanced variability. Mean meridional winds even have different directions in different years: In 2012 it is mainly northward, in 2014 it has no predominant direction, and in 2015 it is mainly southward.

~~Concluding from these remarkable differences~~Besides this noticeable year-to-year variations we find large variability within the Januaries of the different years. The standard deviations of temperature data at 50 km respectively 70 km altitude are 6 K and 21 K in January 2012, 8 K and 7 K in January 2014, and 4 K and 9 K in January 2015; noteworthy is the increased standard deviation of 18 K at 60 km altitude in January 2015. The standard deviations of zonal and meridional wind data are of nearly same size ($\pm 2\,\mathrm{m\,s^{-1}}$), namely at 50 km respectively 70 km altitude: $18\,\mathrm{m\,s^{-1}}$ and $29\,\mathrm{m\,s^{-1}}$ in January 2012, $24\,\mathrm{m\,s^{-1}}$ and $26\,\mathrm{m\,s^{-1}}$ in January 2014, and $20\,\mathrm{m\,s^{-1}}$ and $30\,\mathrm{m\,s^{-1}}$ in January 2015.

Concluding from the remarkable year-to-year variations and variabilities within Januaries of different years: The polar middle atmosphere in January cannot be described by one single "winter state", and it is not appropriate to infer a general statement or even a climatology from observations of only a few seasons. To investigate the variations in one single month an example is shown in the next section.

4.2 Elevated stratopause and polar-vortex reformation after minor SSW in January 2012

During winters, variability in the polar middle atmosphere is mainly caused by planetary waves and sudden stratospheric warmings (SSW): Depending on their type and strength, the polar vortex may be weakened, displaced, or even split~~,~~; warmer air from mid-latitudes may intrude into the polar region (e.g., Matsuno, 1971; Labitzke, 1972). The number of SSWs during one season and the time at which they appear vary from year to year (e.g., Labitzke and Kunze, 2012). Around 15 January 2012 a minor SSW, which was a vortex displacement event, occurred (Chandran et al., 2013; Matthias et al., 2013). The ALOMAR RMR lidar has taken data during the following days and weeks, i.e., the aftermath of the SSW. Figure 2 shows the temporal evolution of temperature and zonal and meridional wind after the SSW, starting on 19 January until 4 February. Except of the double-stratopause structure, the temperature profiles from 19 January do not look unusual; the temperature increase between 70 and 80 km altitude indicates a mesospheric inversion layer, whose investigation is, however, beyond the scope of this study. Though, the westward zonal winds are exceptional for winter, which is probably a result of the vortex displacement. ~~Only~~ The strength and relative position of the polar vortex can be inferred from the potential vorticity: Rex et al. (1998) define 36 PVU at the 475 K potential temperature level as the edge of the polar vortex. Basing on this definition and using potential vorticity and potential temperature from ECMWF data, ALOMAR is situated inside the polar vortex during that night. It has to be kept in mind that the polar vortex might bend and twist and therefore the vortex location as defined at 475 K (≈ 19 km altitude) may not always represent the situation in the upper strato- and mesosphere. Only a few days later (21/22 and 22/23 January) the stratopause is ~~some~~ ≈ 15 to 20 K colder and the upper mesosphere around 70 km altitude is ~~some~~ ≈ 15 to 20 K warmer; zonal winds are now ~~weak~~ weakly eastward over the entire altitude range and meridional winds are developing from ~~weak southward toward weak northward , also~~ weakly southward toward weakly northward with only small ~~vertical variability.~~ variations in altitude. In the first of these two nights the polar vortex edge was above ALOMAR, while in the second night ALOMAR was situated outside the vortex. Baumgarten et al. (2015) show time-altitude sections of temperature and wind data of this period, which exhibit very pronounced gravity wave structures. During the following week, the thermal and dynamic structure over

ALOMAR changed remarkably: The temperature maximum around 40 km altitude vanished, highest temperatures occur now (28/29 and 29/30 January) around 70 km altitude; at roughly the same altitude maxima of zonal and meridional wind occur. ALOMAR was again situated inside the polar vortex. During beginning of February the maxima in temperature, zonal and meridional wind even intensify and descend further down. These phenomena are closely connected to the preceding SSW: They are referred to as elevated stratopause and reformation of the polar vortex, which sometimes occur after stratospheric warmings (e.g., Labitzke, 1972; Manney et al., 2009). In contrast to the present study, these two studies analyzed vortex split events with a complete breakdown of the polar vortex.

Concluding, the minor SSW of 2012 is peculiar: It is followed by an elevated stratopause event, although it is neither a major warming nor a vortex split event. Thus, this SSW is an example ~~,~~ that elevated stratopause events can occur even after minor SSW, as previously stated by de la Torre et al. (2012) and Chandran et al. (2013). Although the basic mechanisms of elevated stratopauses and the polar vortex reformation are known (e.g., Tomikawa et al., 2012) and temperatures and zonal mean zonal winds were derived previously (winds only indirectly from geopotential-height observations by satellites (e.g., Manney et al., 2009)), this is the first time that an elevated stratopause together with the reformation of the polar vortex were observed with a direct temperature and wind measurement technique. These unique observations reveal features which are not ~~visible~~ represented in ECMWF data, which highlights the need for observations of such peculiar events to broaden the data basis against which models can be compared to test their fidelity. The differences, which are present in temperature and wind data as well, highlight the importance of local observations with adequate spatial and temporal resolution, and will be discussed in detail in the following section.

4.3 Comparison to models

Figure 2 includes data extracted from ECMWF. Especially above 50 km altitude the comparison between lidar and ECMWF is dissatisfying, particularly for end of January and beginning of February: The elevated stratopause and the reformation of the polar vortex are not captured sufficiently in ECMWF. This yields to differences of up to 40 K and 20 $\mathrm{m\,s^{-1}}$, respectively. One explanation for the poor comparison might be that this period was affected by an SSW. Therefore, we study the comparison of lidar data with ECMWF and HWM07 data for the whole data set, which is shown in Fig. 3: It depicts the same lidar profiles as Fig. 1 and mean profiles taken from ECMWF for January 2012 (panel a), January 2014 (b), and January 2015 (c), and data cumulated over all three seasons, including ~~HMW07~~HWM07 (d). Note ~~,~~ that all three data sets have the same temporal sampling. The standard deviation is calculated as the deviation of all 1 h profiles of one month from the ~~month-mean~~ monthly mean profile, which is calculated from these 1 h profiles.

We first concentrate on HWM07 data (panel d, winds only). Although HWM07 is more like a climatology without any year-to-year variation, some studies use it as representation of mean or background wind fields ~~(e.g., Assink et al., 2012; Hedlin and Walker, 201~~ even for single case studies, (e.g., Assink et al., 2012; Hedlin and Walker, 2012; Fee et al., 2013). However, HWM07 describes the actual winds insufficiently: Zonal wind is too weak in the upper stratosphere (compared to ECMWF) and too strong in the upper mesosphere (compared to lidar), differences are up to 20 $\mathrm{m\,s^{-1}}$; in between mean zonal wind matches quite well. HWM07's meridional wind is too strong in the entire altitude range covered; differences are on the order of 30 $\mathrm{m\,s^{-1}}$.

The temporal variability (indicated by the standard deviation) is much smaller than for the lidar data. One reason for this ~~discrepancies~~discrepancy, aside from the missing year-to-year variations in HWM07, is the limited number of observations taken into account in HWM07 for this location and altitude range~~.~~ (see Tab. 1 in Drob et al. (2008)).

Comparison with ECMWF data: The data of 2014 and 2015 were not affected by SSWs, but still the temperature comparison between lidar and ECMWF is not good: The stratopause is too cold (up to 10 K) and too low (up to 4 km) in ECMWF; at higher altitudes temperatures from ECMWF are ~~way too low~~much too low, namely up to 25 K. This can also be seen in panel (a) of Fig. 4, which shows altitude profiles of the mean of the hourly differences ($\Delta x = \frac{1}{N}\sum(x_{\mathrm{ECMWF}} - x_{\mathrm{lidar}})$), including the respective standard deviation and the standard error of the mean for the lidar data. ~~Temperature differences between lidar and ECMWF are up to 20 K above 65 km altitude.~~Regarding zonal winds, the comparison between ECMWF and lidar is nonuniform for the three years: In 2012 and 2014 it is ~~good~~ very good with mean differences of only around 2 m s^{-1} or even smaller below 60 km altitude~~but mean differences rise~~ ; above, mean differences are up to 20 m s^{-1}, respectively 15 m s^{-1}~~above~~; in 2015 mean differences between 10 and 20 m s^{-1} occur in the entire altitude range between 45 and 70 km. For meridional winds the comparison is ~~slightly~~ much better: Mean differences are mostly smaller or around 5 m s^{-1} only, hence on the same order as the standard error of the mean of the lidar data. Similar results concerning ECMWF temperatures in the middle and upper mesosphere were reported by, e.g., Le Pichon et al. (2015). They state that the wave-like pattern of the differences profile might be caused by a quasi-stationary planetary wave structure. A study by Rüfenacht et al. (2014) applying wind radiometry found good agreement of observed winds and ECMWF wind data in the stratosphere, but ~~some~~ deviations in the mesosphere ~~.~~ of up to 50% of the true wind speeds. Please note that the ECMWF IFS cycles used in these studies differ from the ones used in this study.

Figure 4(b) shows distributions of differences on hourly basis for different altitude ranges. The distributions of differences are getting broader for higher altitudes; some distributions are not symmetrical, indicating systematic under- or overestimations for the respective measure. This is especially true for temperatures and zonal winds above 50 km altitude; but does not appear for meridional winds in the entire altitude range covered.

This leads to studying the comparison of lidar and ECMWF data on shorter time scales: Figure 5 shows all 1 h profiles of temperature, zonal, and meridional wind speed, derived by lidar during the night 20/21 January 2015 (between 14:40 UTC and 07:30 UTC) and extracted from ECMWF corresponding to the temporal sampling of the lidar (and interpolated to the vertical resolution of the lidar data). Despite the differences between the mean lidar and ECMWF profiles, it is obvious that the lidar data show a larger variability in altitude and time. These differences on smaller scales are the reason for the width of the distribution of differences shown in Fig. 4(b). Despite the differences of single 1 h profiles or ~~night-mean~~ nightly mean profiles in principle, the smaller temporal and vertical variability in ECMWF data might indicate that the amount of energy and momentum which is transported by waves is underestimated in ECMWF, which might cause part of the discrepancies of the mean state as shown in Fig. 4(a).

To study the comparison of the variability of each data set in more detail, the dashed lines in Fig. 5 show the ~~RMS of the~~ root mean square (RMS) of the fluctuations of the 1 h profiles, hence their variability. The RMS of the lidar data increases with altitude, indicating an increase of the amplitudes of the temperature and wind fluctuations (note that the RMS increases faster and is always larger than the mean measurement uncertainty of the lidar data). This is what is expected for the effect of gravity waves, as their amplitudes increase with altitude due to the decreasing air density. In contrast, the RMS profiles of the ECMWF data do not show a general increase with altitude and in large part of the altitude range the RMS of the ECMWF data is smaller than the RMS of the lidar data. This is also true for the whole data set, as can be seen in Fig. 4(c): For each night with at least ten hours of data the RMS of the lidar data and the RMS of the ECMWF data are calculated, then the ~~month-average~~ monthly average of the ratio of both is calculated and drawn. In general, the higher in altitude the worse is the actual variability represented in ECMWF, down to only one tenth; one exception is the temperature in January 2012, when the ECMWF ~~variabiliy~~ variability even at high altitudes is about one third of the lidar variability. Similar results regarding the ~~height dependent~~ height-dependent underestimation of gravity wave amplitudes were also reported by Schroeder et al. (2009): From a comparison of model data with global satellite observations they infer that temperature amplitudes in ECMWF are underestimated by a factor of 2 at 28 km altitude and more than five times above 40 km altitude. The reason for the underestimation of the variability at higher altitudes are likely damping mechanisms that are applied in the ECMWF model; an extensive overview of several such approaches is given by Jablonowski and Williamson (2011).

Concluding, ECMWF and especially HWM07 do not represent ~~sufficiently~~ the thermal and dynamic state of the middle atmosphere sufficiently, regarding January-mean profiles and the variability within single nights, which is underestimated in ECMWF data. This distinct underestimation of the temporal variability of temperatures and winds affects the energy budget of gravity waves which are the main source ~~for~~ of fluctuations on the scale of a few hours. Resulting gravity wave energy densities will be discussed in the next section.

4.4 ~~Gravity-wave~~ Gravity wave energy density

The combination of simultaneous wind and temperature measurements allows to perform wave studies in more detail. For instance, the energy budget of gravity waves consists of potential and kinetic gravity wave energy; while the former depends on the temperature fluctuations, the latter is based on the wind speed fluctuations. We used the following equations (e.g., Geller and Gong, 2010) to derive potential and kinetic gravity wave energy density (GWED) per unit mass from temperature and wind speed fluctuations (T', u', and v', respectively):

$$E_{\text{pot}} = \frac{1}{2}\frac{g^2}{N^2}\left(\frac{T'}{\bar{T}}\right)^2 \qquad \text{and} \qquad E_{\text{kin}} = \frac{1}{2}\left({u'}^2 + {v'}^2\right), \quad (1)$$

with g as gravitational acceleration, N as Brunt–Väisälä frequency, and $\bar{T}$ as background temperature. The fluctuations are derived by subtracting the respective ~~night-mean~~ nightly mean profile. As stated by Ehard et al. (2015), applying this method might include tidal signatures in the resulting gravity wave energy densities; furthermore, the resolved GW spectrum depends on the length of an observation, which hinders comparison of GWEDs. Although Ehard et al. (2015) proposed applying a Butterworth filter to extract GWs, we use the ~~night-mean~~ nightly mean method since we tested different approaches for background estimation with our lidar data and found no significant differences in the resulting GWEDs. To accommodate the mentioned drawbacks of the ~~night-mean~~ nightly mean method, we apply the following procedure: We take only measurements with at least 10 h duration into account (since the ~~night-mean~~ nightly mean profiles of shorter measurements would include wave-like features); within one night we then select the first ten 1 h profiles to calculate GWEDs for this time span (therefore, the covered GW spectrum is relatively wide and constant for all observations, although it might contain some short-scale tidal components); we shift the 10 h window by 1 h and repeat the GWED calculation as often as the window fits into the observation period of that night (therefore, different phases of possibly included tides are sampled); finally we calculate the mean and the standard deviation of all the GWED profiles of one night (therefore, we can estimate the GWED variability during single nights). As an example, the left panel of Fig. 6 shows vertical profiles of potential and kinetic GWED for the night 20/21 January 2015. Except at around 47 km and 52 km altitude, the kinetic GWED is larger than the potential GWED, mostly four to five times (shown in the right panel of Fig. 6). As expected from Eq. (1) the potential GWED shows minima and maxima at the same altitudes as the minima and maxima of the temperature fluctuations (cf. Fig. 5); while the kinetic GWED correlates to features of zonal and meridional wind fluctuations (e.g., the minimum of kinetic GWED at 67 km altitude).

The middle panel of Fig. 6 shows the total GWED. Between 47 and 53 km altitude, and above 67 km the total GWED increases with altitude. In between is a layer of slightly decreasing total GWED, caused mainly by the decrease of potential GWED. A possible reason might be the near adiabatic temperature gradient between 50 and 60 km altitude (some profiles show gradients of $\approx -7\,\mathrm{K\,km^{-1}}$), which hinders the upward propagation of gravity waves.

The right panel of Fig. 6 shows the ratio of kinetic to potential GWED and the intrinsic period $2\pi\hat{\omega}^{-1}$ ~~of the gravity wave ensemble, as calculated from the kinetic-to-potential GWED ratio for low- and medium-frequency waves~~that a monochromatic low- or medium-frequency gravity wave with the given E_{pot} and E_{kin} would have (Geller and Gong, 2010):

$$\hat{\omega} = \pm f\sqrt{\frac{E_{\mathrm{kin}}/E_{\mathrm{pot}}+1}{E_{\mathrm{kin}}/E_{\mathrm{pot}}-1}}, \tag{2}$$

with the Coriolis parameter $f = 2\Omega\sin\phi$ (Ω: angular speed of Earth's rotation, ϕ: latitude of observation). We have shown earlier that at times of quasi-monochromatic waves the intrinsic periods calculated from the energy ratios agree to the results of the hodograph method (Baumgarten et al., 2015). ~~Compared to~~ While the hodograph method ~~, this approach using energy ratios has the advantage that an (energy weighted) intrinsic period for the ensemble of waves~~ can only be applied in the case of a quasi-monochromatic wave – because it would otherwise be hard or even impossible to identify an ellipse from the zonal and meridional wind fluctuations –, the energy ratio method is applicable also to wind and temperature fluctuations caused by various waves, keeping in mind that the derived $2\pi\hat{\omega}^{-1}$ is not the intrinsic period of a certain wave. However, the method has been applied previously to data sets probably affected by superposition of various gravity waves (e.g., Geller and Gong, 2010; Baumgarten e
Note that since temperature and horizontal wind fluctuations are more sensitive to long-period gravity waves than to short-period gravity waves, the energy ratio method is biased toward long-period gravity waves, as stated by Lane et al. (2003) and evaluated by Geller and Gong (2010, their App. A). Nevertheless, due to the temporal integration of the data, short-period gravity waves are discarded anyway. The retrieved $2\pi\hat{\omega}^{-1}$ is ~~calculated. The intrinsic period is~~ larger than 8 h in most parts; highest values are about 11 h, reasonably smaller than the upper limit of $2\pi f^{-1} = 12.82\,\mathrm{h}$. According to the relationship for the group velocity vector (e.g., Fritts and Alexander, 2003)

$$(c_{\mathrm{g}x}, c_{\mathrm{g}y}, c_{\mathrm{g}z}) = (\bar{u}, \bar{v}, 0) + \frac{[k(N^2-\hat{\omega}^2), l(N^2-\hat{\omega}^2), -m(\hat{\omega}^2-f^2)]}{\hat{\omega}\left(k^2+l^2+m^2+\frac{1}{4H^2}\right)}, \tag{3}$$

with k, l, m as zonal, meridional, and vertical wave number, respectively, this indicates a more horizontal wave propagation, as $\hat{\omega}^2 - f^2 \to 0$ (and $\hat{\omega}^2 \ll N^2$). The two pronounced minima of ~~the intrinsic period~~ $2\pi\hat{\omega}^{-1}$ around 46 km and 53 km altitude are caused by equality of potential and kinetic GWED; wind fluctuations are quite low at these altitudes, while the temperature fluctuations are quite large. This then indicates waves which propagate more vertically, as the weight of $N^2 - \hat{\omega}^2$ in Eq. (3) decreases and the weight of $\hat{\omega}^2 - f^2$ increases. The different vertical-to-horizontal propagation conditions at 46 km and 53 km compared to the remaining altitude ranges may be caused by different reasons: 1. different origin of the waves; 2. changing background propagation conditions, i.e., filtering/Doppler shift due to the strong zonal wind shear in this altitude range from $80\,\mathrm{m\,s^{-1}}$ to $20\,\mathrm{m\,s^{-1}}$. A clear distinction of both possible explanations is not possible: While the second option is clearly visible in Fig. 5 (large temperature gradient and strong wind shear), the first option can not be excluded. However, a detailed investigation of propagation conditions is beyond the scope of this study.

Figure 6 includes also GWEDs and the ~~intrinsic period of the GW ensemble derived from ECWMF~~ $2\pi\hat{\omega}^{-1}$ derived from ECMWF data for the same time period. In the lower part (up to ≈ 50 km altitude), the GWEDs are comparable to the lidar data. Above, the total GWED derived from ECMWF data decreases with altitude. Therefore, at 70 km altitude the GWEDs derived from ECMWF data are nearly two orders of magnitude too small. The kinetic-to-potential GWED ratio is on the same order as the GWED ratio derived by lidar, although the shapes differ, yielding differing profiles of ~~intrinsic period~~$2\pi\hat{\omega}^{-1}$.

Are these results special or typical? Figure 7 shows mean GWEDs for January 2012, 2014, and 2015, derived from lidar (panel a) and ECMWF data (panel b). For this, altitude profiles of GWED of all nights with at least 10 h of data were averaged. Comparing Figs. 6 and 7(a), the data from 20/21 January 2015 is not unusual. Although the mean total GWED of January 2015 increases in nearly the entire altitude range (in contrast to the data of 20/21 January 2015), the increase is slightly larger below ≈ 55 km altitude than above. The same is true for January 2014. In January 2012 the GWED between 40 and 60 km altitude is somewhat smaller than in January 2014 and 2015. The increase of total GWED with altitude exhibits a scale height of ≈ 16 km. This is 2.3 times larger than the pressure scale height of 7 km; a relation previously obtained by Fritts and VanZandt (1993) by posing a model gravity wave spectrum. The same scale height was found by Kaifler et al. (2015), although they observed potential energy densities only. Similar scale heights for total energy density and potential energy density would imply a kinetic-to-potential GWED ratio constant with altitude. However, our observations show that the kinetic-to-potential GWED ratio is typically between 5 and 10 and slightly increases with altitude, as can be seen in the right panel of Fig. 7(a). When comparing absolute values of GWED to previous studies it is necessary to keep in mind, that GWEDs depend on season, locally different wave sources, and data analysis procedures (e.g., Baumgarten et al., 2017). Nevertheless, studies by Alexander et al. (2011) and Mzé et al. (2014) at Antarctic and mid-latitude stations, respectively, found quantitatively similar results for potential GWEDs averaged over multiple years. Comparing data obtained at high-latitude stations is further affected by the position of the polar vortex, as shown by Whiteway et al. (1997).

Looking at mean GWEDs derived from ECMWF, below 45 km altitude they are of similar order as the mean total GWEDs derived from lidar data. Above, the mean GWEDs derived from ECMWF are more or less constant with altitude, yielding an underestimation of GWED in ECMWF by factor 3 to 10. This is in line with the underestimated temporal temperature and wind speed variability found in Sect. 4.3.

Applying the method to calculate energy densities not on 1 h profiles but on all ~~night-mean~~ nightly mean temperature and wind speed profiles of one month yields energy densities on a larger time scale. Taking into account only nights with at least 10 h of observations largely reduces the effect of gravity waves and highlights the contribution from planetary waves or diurnal tides. It has to be noted that applying Eq. (1) to such large-scale variations assumes vertical displacements to be adiabatic and periodic, and advection is neglected. Analogous to the term gravity wave energy density (GWED) we will use the term large-scale wave energy densitiy (LWED) to denote the so derived energy densities. The results for January 2012, January 2014, and January 2015 are shown in Fig. 8, for lidar data (panel a) and ECMWF data (panel b). Compared to GWED, potential and kinetic LWEDs are more variable with altitude and it occurs more often, that potential LWED is larger than kinetic LWED. Therefore, kinetic-to-potential LWED ratios vary over more than two orders of magnitude. Although total LWEDs show distinct vertical variations, the overall increase with altitude is rather small: It slightly increases in January 2012 (with a local maximum around 70 km altitude) and January 2014 and slightly decreases in January 2015 with a local maximum around 60 km altitude. Contrary to GWED, total LWED derived from ECMWF data is roughly of the same order of magnitude as the total LWED obtained from lidar data, not only in the lower part but in the entire altitude range; e.g., at 61 km altitude mean total LWEDs range from $\approx 2.2 \cdot 10^2\,\mathrm{J\,kg^{-1}}$ to $\approx 7.3 \cdot 10^2\,\mathrm{J\,kg^{-1}}$ for the lidar data and from $\approx 1.7 \cdot 10^2\,\mathrm{J\,kg^{-1}}$ to $\approx 2.4 \cdot 10^2\,\mathrm{J\,kg^{-1}}$ for the ECMWF data. The kinetic-to-potential energy ratio is larger for the ECMWF data compared to lidar data; especially above 55 km altitude. The explanation is that while the kinetic LWEDs derived from lidar data and ECMWF data are of the same order, the potential LWEDs derived from ECMWF data are smaller than derived from lidar data. Hence, the day-to-day variability of temperatures in ECMWF is too weak, which is visible in Fig. 2 for January 2012.

Comparison of GWED and LWED profiles shows that LWEDs are mainly on the same order of magnitude as GWEDs. Increased mean LWED-to-GWED ratios (up to 10) occur between 60 km and 70 km altitude and below 50 km altitude for potential energy densities, and below 50 km altitude for kinetic energy densities, as is shown in Fig. 9.

The total LWED is about 2 to 6 times larger than the total GWED.

5 Summary and conclusions

We presented results of more than 300 h of simultaneous temperature and wind observations by Doppler lidar in the Arctic stratosphere and mesosphere, ranging from 30 up to about 85 km altitude, obtained during Januaries 2012, 2014, and 2015.

Considering only these three years, large variability in the mean temperatures and horizontal winds is observed. The temperature and wind data were affected by ~~large scale~~ large-scale dynamics in the middle atmosphere, e.g., an SSW in January 2012. After this minor SSW, two phenomena that are commonly linked to major SSWs (in particular polar vortex split events) were observed by the ALOMAR RMR lidar: an elevated stratopause and the reformation of the polar vortex. This large-scale activity can ~~for example be seen~~ be seen for example in the LWED for January 2012 at about 70 km altitude when comparing to altitudes below or the Januaries 2014 and 2015.

We compared mean temperatures and winds from lidar observations to ECMWF and HWM07 data, where we used model data only at times of the lidar observations. ~~We~~ Below $\approx 55\,\mathrm{km}$ altitude monthly mean zonal and meridional winds derived from lidar observations and extracted from ECMWF model data agree very well, with differences smaller than $2\,\mathrm{m\,s^{-1}}$ and $5\,\mathrm{m\,s^{-1}}$, respectively. Above, we found differences of up to $20\,\mathrm{K}$, $20\,\mathrm{m\,s^{-1}}$, and $5\,\mathrm{m\,s^{-1}}$ for ~~month-mean~~ monthly mean profiles of temperature, zonal, and meridional wind, respectively, between lidar and ECMWF data and of up to $30\,\mathrm{m\,s^{-1}}$ between lidar and HWM07 data.

Analysis of monthly mean gravity wave energy densities showed an increase of total GWED per unit mass with altitude with a scale height of $\approx 16\,\mathrm{km}$, which agrees with previously published values. From the ratio of kinetic to potential GWED (which is typically 5 to 10) the intrinsic period ~~of the GW ensemble of~~ that a monochromatic gravity wave with the given energy densities would have is deduced for one exemplary night~~is deduced~~, which varies remarkably with altitude. These ~~different intrinsic periods~~ variations of $\hat{\omega}$ might be caused by diverse origins of the waves or changing background conditions for wave propagation. Comparison with ECMWF data ~~show~~ shows that GWEDs are underestimated in ECMWF by factor 3 to 10 above $50\,\mathrm{km}$ altitude. Analyzing fluctuations of ~~night-mean~~ nightly mean profiles allows a similar study for large-scale waves instead of gravity waves. Compared to GWEDs, the LWEDs show larger vertical variations but the overall increase with altitude is smaller. Contrary to GWEDs, the kinetic-to-potential LWED ratios might become smaller 1, this indicates more variability in temperature than in wind, which applies for the remarkable temperature changes in January 2012 at $40\,\mathrm{km}$ and $70\,\mathrm{km}$ altitude in the course of the SSW (cf. Fig. 2). Likewise, a ratio larger 1 indicates larger wind speed variability, e.g., in January 2014 and January 2015 around $50\,\mathrm{km}$ altitude, when the stratopause temperature is quite stable while wind speeds vary strongly (they are affected sensitively by the shape and position of the polar vortex). Total LWEDs derived from ECMWF data agree reasonably well to LWEDs derived from lidar data: E.g., at $61\,\mathrm{km}$ altitude the mean LWEDs derived from lidar and ECMWF data are $\approx 4.5 \cdot 10^2\,\mathrm{J\,kg^{-1}}$ and $\approx 2.0 \cdot 10^2\,\mathrm{J\,kg^{-1}}$, respectively. LWEDs are mainly on the same order of magnitude as GWEDs. ~~In~~ Alt altitudes of enhanced large-scale variations, namely between $60\,\mathrm{km}$ and $70\,\mathrm{km}$ altitude for temperatures and below $50\,\mathrm{km}$ altitude for winds, they exceed GWEDs by up to 10. The total LWED is about 2 to 5 times larger than the total GWED.

In future studies daylight data will be included, which will allow to capture tidal effects ~~,~~ and extend the analyses to other seasons.

Acknowledgements. This study benefited from the excellent support by the dedicated staff at the ALOMAR observatory and the voluntary lidar operators during winter campaigns. The European Centre for Medium-Range Weather Forecasts (ECMWF) is gratefully acknowledged for providing the ~~operational analysis~~ forecast data; cycles ~~Cy36r1 and Cy38r2~~ Cy37r3 and Cy40r1 were used in this study. The DoRIS project was supported by Deutsche Forschungsgemeinschaft (DFG, German Research Foundation, No. BA 2834/1-1). This project has received funding from the European Union's Horizon 2020 Research and Innovation programme under grant agreement No. 653980 (ARISE2), and was supported by the Deutsche Forschungsgemeinschaft (DFG, German Research Foundation) under project No. LU 1174 (PACOG) and by the German Federal Ministry of Education and Research through the program Role Of The Middle atmosphere In Climate (ROMIC).

References

Alexander, S. P., Klekociuk, A. R., and Murphy, D. J.: Rayleigh lidar observations of gravity wave activity in the winter upper stratosphere and lower mesosphere above Davis, Antarctica (69°S, 78°E), J. Geophys. Res., 116, n/a–n/a, doi:10.1029/2010JD015164, http://dx.doi.org/10.1029/2010JD015164, d13109, 2011.

Assink, J. D., Waxler, R., and Drob, D.: On the sensitivity of infrasonic traveltimes in the equatorial region to the atmospheric tides, J. Geophys. Res., 117, n/a–n/a, doi:10.1029/2011JD016107, http://dx.doi.org/10.1029/2011JD016107, d01110, 2012.

Baron, P., Murtagh, D. P., Urban, J., Sagawa, H., Ochiai, S., Kasai, Y., Kikuchi, K., Khosrawi, F., Körnich, H., Mizobuchi, S., Sagi, K., and Yasui, M.: Observation of horizontal winds in the middle-atmosphere between 30° S and 55° N during the northern winter 2009–2010, Atmos. Chem. Phys., 13, 6049–6064, doi:10.5194/acp-13-6049-2013, http://www.atmos-chem-phys.net/13/6049/2013/, 2013.

Baumgarten, G.: Doppler Rayleigh/Mie/Raman lidar for wind and temperature measurements in the middle atmosphere up to 80 km, Atmos. Meas. Tech., 3, 1509–1518, 2010.

Baumgarten, G., Fiedler, J., Hildebrand, J., and Lübken, F.-J.: Inertia gravity wave in the stratosphere and mesosphere observed by Doppler wind and temperature lidar, Geophys. Res. Lett., 42, 10,929–10,936, doi:10.1002/2015GL066991, http://dx.doi.org/10.1002/2015GL066991, 2015GL066991, 2015.

Baumgarten, K., Gerding, M., and Lübken, F.-J.: Seasonal variation of gravity wave parameters using different filter methods with daylight lidar measurements at mid-latitudes, J. Geophys. Res., accepted, 2017.

Bossert, K., Fritts, D. C., Pautet, P.-D., Taylor, M. J., Williams, B. P., and Pendelton, W. R.: Investigation of a mesospheric gravity wave ducting event using coordinated sodium lidar and Mesospheric Temperature Mapper measurements at ALOMAR, Norway (69°N), J. Geophys. Res., 119, 9765–9778, doi:10.1002/2014JD021460, http://dx.doi.org/10.1002/2014JD021460, 2014JD021460, 2014.

Chandran, A., Collins, R. L., Garcia, R. R., Marsh, D. R., Harvey, V. L., Yue, J., and de la Torre, L.: A climatology of elevated stratopause events in the whole atmosphere community climate model, J. Geophys. Res., 118, 1234–1246, doi:10.1002/jgrd.50123, http://dx.doi.org/10.1002/jgrd.50123, 2013.

Chandran, A., Garcia, R. R., Collins, R. L., and Chang, L. C.: Secondary planetary waves in the middle and upper atmosphere following the stratospheric sudden warming event of January 2012, Geophys. Res. Lett., 40, 1861–1867, doi:10.1002/grl.50373, 2013.

Chanin, M. L. and Hauchecorne, A.: Lidar Observation of Gravity and tidal Waves in the Stratosphere and Mesosphere, Geophys. Res. Lett., 86, 9715–9721, 1981.

de la Torre, L., Garcia, R. R., Barriopedro, D., and Chandran, A.: Climatology and characteristics of stratospheric sudden warmings in the Whole Atmosphere Community Climate Model, J. Geophys. Res., 117, n/a–n/a, doi:10.1029/2011JD016840, http://dx.doi.org/10.1029/2011JD016840, 2012.

Dörnbrack, A., Gisinger, S., and Kaifler, B.: On the Interpretation of Gravity Wave Measurements by Ground-Based Lidars, Atmosphere, 8, doi:10.3390/atmos8030049, http://www.mdpi.com/2073-4433/8/3/49, 2017.

Drob, D. P., Emmert, J. T., Crowley, G., Picone, J. M., Shepherd, G. G., Skinner, W., Hays, P., Niciejewski, R. J., Larsen, M., She, C.-Y., Meriwether, J. W., Hernandez, G., Jarvis, M. J., Sipler, D. P., Tepley, C. A., O'Brien, M. S., Bowman, J. R., Wu, Q., Murayama, Y., Kawamura, S., Reid, I. M., and Vincent, R. A.: An empirical model of the Earth's horizontal wind fields: HWM07, J. Geophys. Res., 2008.

Eckermann, S. D., Hirota, I., and Hocking, W. K.: Gravity wave and equatorial wave morphology of the stratosphere derived from long-term rocket soundings, Quart. J. R. Met. Soc., 121, 149–186, doi:10.1002/qj.49712152108, http://dx.doi.org/10.1002/qj.49712152108, 1995.

Ehard, B., Kaifler, B., Kaifler, N., and Rapp, M.: Evaluation of methods for gravity wave extraction from middle-atmospheric lidar temperature measurements, Atmos. Meas. Tech., 8, 4645–4655, doi:10.5194/amt-8-4645-2015, http://www.atmos-meas-tech.net/8/4645/2015/, 2015.

Fee, D., Waxler, R., Assink, J., Gitterman, Y., Given, J., Coyne, J., Mialle, P., Garces, M., Drob, D., Kleinert, D., Hofstetter, R., and Grenard, P.: Overview of the 2009 and 2011 Sayarim Infrasound Calibration Experiments, J. Geophys. Res., 118, 6122–6143, doi:10.1002/jgrd.50398, http://dx.doi.org/10.1002/jgrd.50398, 2013.

Franke, S. J., Chu, X., Liu, A. Z., and Hocking, W. K.: Comparison of meteor radar and Na Doppler lidar measurements of winds in the mesopause region above Maui, Hawaii, J. Geophys. Res., 110, D09S02, doi:10.1029/2003JD004486, 2005.

Friedman, J. S., Tepley, C. A., Castleberg, P. A., and Roe, H.: Middle-atmospheric Doppler lidar using an iodine-vapor edge filter, Opt. Lett., 22, 1648–1650, 1997.

Fritts, D. C. and Alexander, M. J.: Gravity wave dynamics and effects in the middle atmosphere, Rev. Geophys., 41, 1003, doi:10.1029/2001RG000106, 2003.

Fritts, D. C. and VanZandt, T. E.: Spectral estimates of gravity wave evergy and momentum fluxes. Part I: Energy dissipation, acceleration, and constraints., J. Atmos. Sci., 50, 3685–3694, doi:10.1175/1520-0469(1993)050<3685:SEOGWE>2.0.CO;2, 1993.

Geller, M. A.: Dynamics of the middle atmosphere, Space Sci. Rev., 34, 359–375, 1983.

Geller, M. A. and Gong, J.: Gravity wave kinetic, potential, and vertical fluctuation energies as indicators of different frequency gravity waves, J. Geophys. Res., 115, n/a–n/a, doi:10.1029/2009JD012266, http://dx.doi.org/10.1029/2009JD012266, 2010.

Gill, A. E.: Atmosphere–Ocean Dynamics, vol. 30 of *International Geophysics Series*, Academic Press, 1982.

Goldberg, R. A., Fritts, D. C., Williams, B. P., Lübken, F.-J., Rapp, M., Singer, W., Latteck, R., Hoffmann, P., Müllemann, A., Baumgarten, G., Schmidlin, F. J., She, C.-Y., and Krueger, D. A.: The MaCWAVE/MIDAS rocket and ground-based measurements of polar summer dynamics: Overview and mean state structure, Geophys. Res. Lett., 31, n/a–n/a, doi:10.1029/2004GL019411, http://dx.doi.org/10.1029/2004GL019411, l24S02, 2004.

Hauchecorne, A. and Chanin, M.-L.: Density and temperature profiles obtained by lidar between 35 and 70 km, Geophys. Res. Lett., 7, 565–568, doi:10.1029/GL007i008p00565, 1980.

Hays, P. B., Abreu, V. J., Dobbs, M. E., Gell, D. A., Grassl, H. J., and Skinner, W. R.: The High-Resolution Doppler Imager on the Upper Atmosphere Research Satellite, J. Geophys. Res., 981, 10 713, doi:10.1029/93JD00409, 1993.

Hedlin, M. A. H. and Walker, K. T.: A study of infrasonic anisotropy and multipathing in the atmosphere using seismic networks, Philosophical Transactions of the Royal Society of London A: Mathematical, Physical and Engineering Sciences, 371, doi:10.1098/rsta.2011.0542, http://rsta.royalsocietypublishing.org/content/371/1984/20110542, 2012.

Hildebrand, J., Baumgarten, G., Fiedler, J., Hoppe, U.-P., Kaifler, B., Lübken, F.-J., and Williams, B. P.: Combined wind measurements in the Arctic middle atmosphere, Atmos. Meas. Tech., 5, 2433–2445, doi:10.5194/amt-5-2433-2012, 2012.

Holton, J. R.: The Influence of Gravity Wave Breaking on the General Circulation of the Middle Atmosphere, J. Atmos. Sci., 40, 2497–2507, doi:10.1175/1520-0469(1983)040<2497:TIOGWB>2.0.CO;2, http://dx.doi.org/10.1175/1520-0469(1983)040<2497:TIOGWB>2.0.CO;2, 1983.

Huang, W., Chu, X., Williams, B. P., Harrell, S. D., Wiig, J., and She, C.-Y.: Na double-edge magneto-optic filter for Na lidar profiling of wind and temperature in the lower atmosphere, Opt. Lett., 34, 199–201, doi:10.1364/OL.34.000199, 2009.

Jablonowski, C. and Williamson, D. L.: The Pros and Cons of Diffusion, Filters and Fixers in Atmospheric General Circulation Models, pp. 381–493, Springer Berlin Heidelberg, Berlin, Heidelberg, doi:10.1007/978-3-642-11640-7_13, http://dx.doi.org/10.1007/978-3-642-11640-7_13, 2011.

Kaifler, B., Kaifler, N., Ehard, B., Dörnbrack, A., Rapp, M., and Fritts, D. C.: Influences of source conditions on mountain wave penetration into the stratosphere and mesosphere, Geophys. Res. Lett., 42, 9488–9494, doi:10.1002/2015GL066465, http://dx.doi.org/10.1002/2015GL066465, 2015GL066465, 2015.

Kent, G. S. and Wright, R. W. H.: A review of laser radar measurements of atmospheric properties, J. Atmos. Terr. Phys., 32, 917–943, 1970.

Killeen, T. L., Wu, Q., Solomon, S. C., Ortland, D. A., Skinner, W. R., Niciejewski, R. J., and Gell, D. A.: TIMED Doppler Interferometer: Overview and recent results, J. Geophys. Res., 111, A10S01, doi:10.1029/2005JA011484, 2006.

Kristoffersen, S. K., Ward, W. E., Brown, S., and Drummond, J. R.: Calibration and validation of the advanced E-Region Wind Interferometer, Atmos. Meas. Tech., 6, 1761–1776, doi:10.5194/amt-6-1761-2013, http://www.atmos-meas-tech.net/6/1761/2013/, 2013.

Labitzke, K.: Temperature Changes in the Mesosphere and Stratosphere Connected with Circulation Changes in Winter, J. Atmos. Sci., 29, 756–766, 1972.

Labitzke, K. and Kunze, M.: Interannual Variability and Trends in the Stratosphere, in: Climate and Weather of the Sun-Earth System (CAWSES): Highlights from a Priority Program, edited by Lübken, F.-J., Springer, Dordrecht, The Netherlands, 2012.

Lane, T. P., Reeder, M. J., and Guest, F. M.: Convectively generated gravity waves observed from radiosonde data taken during MCTEX, QJRMS, 129, 1731–1740, doi:10.1256/qj.02.196, http://dx.doi.org/10.1256/qj.02.196, 2003.

Le Pichon, A., Assink, J. D., Heinrich, P., Blanc, E., Charlton-Perez, A., Lee, C. F., Keckhut, P., Hauchecorne, A., Rüfenacht, R., Kämpfer, N., Drob, D. P., Smets, P. S. M., Evers, L. G., Ceranna, L., Pilger, C., Ross, O., and Claud, C.: Comparison of co-located independent ground-based middle atmospheric wind and temperature measurements with numerical weather prediction models, J. Geophys. Res., 120, 8318–8331, doi:10.1002/2015JD023273, http://dx.doi.org/10.1002/2015JD023273, 2015JD023273, 2015.

Lindzen, R. S.: Turbulence and stress owing to gravity wave and tidal breakdown, J. Geophys. Res., 86, 9707–9714, 1981.

Liu, A. Z., Hocking, W. K., Franke, S. J., and Thayaparan, T.: Comparison of Na lidar and meteor radar wind measurements at Starfire Optical Range, NM, USA, J. Atmos. Solar-Terr. Phys., 64, 31–40, doi:10.1016/S1364-6826(01)00095-5, 2002.

Lübken, F.-J. and Müllemann, A.: Temperatures, densities, and winds in the high latitude (78°N) mesosphere, Adv. Space Res., 32, 731–740, doi:10.1016/S0273-1177(03)00408-3, 2003.

Lübken, F.-J., Baumgarten, G., Hildebrand, J., and Schmidlin, F. J.: Simultaneous and co-located wind measurements in the middle atmosphere by lidar and rocket-borne techniques, Atmos. Meas. Tech., 9, 3911–3919, doi:10.5194/amt-9-3911-2016, http://www.atmos-meas-tech.net/9/3911/2016/, 2016.

Manney, G. L., Schwartz, M. J., Krüger, K., Santee, M. L., Pawson, S., Lee, J. N., Daffer, W. H., Fuller, R. A., and N. J. Livesey, N.: Aura Microwave Limb Sounder observations of dynamics and transport during the record-breaking 2009 Arctic stratospheric major warming, Geophys. Res. Lett., 36, doi:10.1029/2009GL038586, 2009.

Matsuno, T.: A Dynamical Model of the Stratospheric Sudden Warming, J. Atmos. Sci., 28, 1479–1494, 1971.

Matthias, V., Hoffmann, P., Manson, A., Meek, C., Stober, G., Brown, P., and Rapp, M.: The impact of planetary waves on the latitudinal displacement of sudden stratospheric warmings, Ann. Geophys., 31, 1397–1415, doi:10.5194/angeo-31-1397-2013, http://www.ann-geophys.net/31/1397/2013/, 2013.

Meriwether, J. W. and Gerrard, A. J.: Mesosphere inversion layers and stratosphere temperature enhancements, Rev. Geophys., 42, RG3003, doi:10.1029/2003RG000133, 2004.

Meyer, W., Philbrick, C. R., Röttger, J., Rüster, R., Widdel, H.-U., and Schmidlin, F. J.: Mean winds in the winter middle atmosphere above northern Scandinavia, J. Atmos. Terr. Phys., 49, 675–687, doi:10.1016/0021-9169(87)90012-2, 1987.

Müllemann, A. and Lübken, F.-J.: Horizontal winds in the mesosphere at high latitudes, Adv. Space Res., 35(11), 1890–1894, 2005.

Mzé, N., Hauchecorne, A., Keckhut, P., and Thétis, M.: Vertical distribution of gravity wave potential energy from long-term Rayleigh lidar data at a northern middle-latitude site, J. Geophys. Res., 119, 12,069–12,083, doi:10.1002/2014JD022035, http://dx.doi.org/10.1002/2014JD022035, 2014JD022035, 2014.

Nappo, C. J.: An introduction to atmospheric gravity waves, Academic Press, 2002.

Placke, M., Hoffmann, P., Gerding, M., Becker, E., and Rapp, M.: Testing linear gravity wave theory with simultaneous wind and temperature data from the mesosphere, J. Atmos. Solar-Terr. Phys., 93, 57–69, doi:http://dx.doi.org/10.1016/j.jastp.2012.11.012, http://www.sciencedirect.com/science/article/pii/S1364682612002854, 2013.

Randel, W. J.: The Evaluation of Winds from Geopotential Height Data in the Stratosphere, J. Atmos. Sci., 44, 3097–3120, 1987.

Rex, M., von der Gathen, P., Harris, N. R. P., Lucic, D., Knudsen, B. M., Braathen, G. O., Reid, S. J., De Backer, H., Claude, H., Fabian, R., Fast, H., Gil, M., Kyrö, E., Mikkelsen, I. S., Rummukainen, M., Smit, H. G., Stähelin, J., Varotsos, C., and Zaitcev, I.: In situ measurements of stratospheric ozone depletion rates in the Arctic winter 1991/1992: A Lagrangian approach, J. Geophys. Res., 103, 5843–5853, doi:10.1029/97JD03127, http://dx.doi.org/10.1029/97JD03127, 1998.

Rüfenacht, R., Kämpfer, N., and Murk, A.: First middle-atmospheric zonal wind profile measurements with a new ground-based microwave Doppler-spectro-radiometer, Atmos. Meas. Tech., 5, 2647, 2012.

Rüfenacht, R., Murk, A., Kämpfer, N., Eriksson, P., and Buehler, S. A.: Middle-atmospheric zonal and meridional wind profiles from polar, tropical and midlatitudes with the ground-based microwave Doppler wind radiometer WIRA, Atmos. Meas. Tech., 7, 4491–4505, doi:10.5194/amt-7-4491-2014, http://www.atmos-meas-tech.net/7/4491/2014/, 2014.

Schmidlin, F. J., Lee, H., and Michel, W.: The Inflatable Sphere: A Technique for the Accurate Measurement of Middle Atmosphere Temperatures, J. Geophys. Res., 96, 22 673–22 682, doi:10.1029/91JD02395, 1991.

Schöch, A., Baumgarten, G., and Fiedler, J.: Polar middle atmosphere temperature climatology from Rayleigh lidar measurements at ALOMAR (69° N), Ann. Geophys., 26, 1681–1698, 2008.

Schroeder, S., Preusse, P., Ern, M., and Riese, M.: Gravity waves resolved in ECMWF and measured by SABER, Geophys. Res. Lett., 36, n/a–n/a, doi:10.1029/2008GL037054, http://dx.doi.org/10.1029/2008GL037054, l10805, 2009.

She, C.-Y., Vance, J. D., Williams, B. P., Krueger, D. A., Moosmuller, H., Gibson-Wilde, D., and Fritts, D.: Lidar studies of atmospheric dynamics near polar mesopause, Trans. Am. Geophys. Union (EOS), 83, 289–, doi:10.1029/2002EO000206, 2002.

Shepherd, G. G., Thuillier, G., Gault, W. A., Solheim, B. H., Hersom, C., Alunni, J. M., Brun, J.-F., Brune, S., Charlot, P., and Cogger, L. L.: WINDII, the wind imaging interferometer on the Upper Atmosphere Research Satellite, J. Geophys. Res., 981, 10 725, doi:10.1029/93JD00227, 1993.

Souprayen, C., Garnier, A., Hertzog, A., Hauchecorne, A., and Porteneuve, J.: Rayleigh-Mie Doppler wind lidar for atmospheric measurements. I: Instrumental setup, validation, and first climatological results, Appl. Optics, 38, 2410–2421, doi:10.1364/AO.38.002410, 1999.

Tepley, C. A.: Neutral winds of the middle atmosphere observed at Arecibo using a Doppler Rayleigh lidar, J. Geophys. Res., 99, 25 781–25 790, doi:10.1029/94JD02213, 1994.

Tomikawa, Y., Sato, K., Watanabe, S., Kawatani, Y., Miyazaki, K., and Takahashi, M.: Growth of planetary waves and the formation of an elevated stratopause after a major stratospheric sudden warming in a T213L256 GCM, J. Geophys. Res., 117, n/a–n/a, doi:10.1029/2011JD017243, http://dx.doi.org/10.1029/2011JD017243, d16101, 2012.

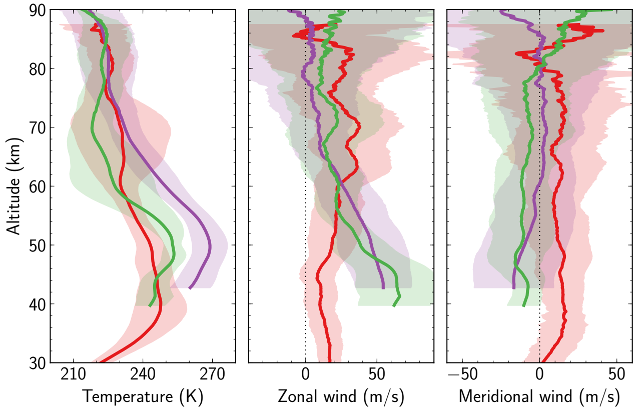

Figure 1. January mean temperatures and horizontal winds derived by lidar for the years 2012 (red), 2014 (purple), and 2015 (green). Shaded areas represent the respective standard deviations.

von Zahn, U., von Cossart, G., Fiedler, J., Fricke, K. H., Nelke, G., Baumgarten, G., Rees, D., Hauchecorne, A., and Adolfsen, K.: The ALOMAR Rayleigh/Mie/Raman lidar: objectives, configuration, and performance, Ann. Geophys., 18, 815–833, 2000.

Whiteway, J. A. and Carswell, A. I.: Lidar observations of gravity wave activity in the upper stratosphere over Toronto, J. Geophys. Res., 100, 14,113–14,124, doi:10.1029/95JD00511, 1995.

Whiteway, J. A., Duck, T. J., Donovan, D. P., Bird, J. C., Pal, S. R., and Carswell, A. I.: Measurements of gravity wave activity within and around the Arctic stratospheric vortex, Geophys. Res. Lett., 24, 1387–1390, doi:10.1029/97GL01322, http://dx.doi.org/10.1029/97GL01322, 1997.

Widdel, H.-U.: Vertical movements in the middle atmosphere derived from foil cloud experiments, J. Atmos. Terr. Phys., 49, 723–741, doi:10.1016/0021-9169(87)90015-8, http://www.sciencedirect.com/science/article/pii/0021916987900158, 1987.

Widdel, H.-U.: Foil chaff clouds as a tool for in-situ measurements of atmospheric motions in the middle atmosphere: Their flight behaviour and implications for radar tracking, J. Atmos. Terr. Phys., 52, 89–101, doi:10.1016/0021-9169(90)90071-T, 1990.

Wu, D. L., Schwartz, M. J., Waters, J. W., Limpasuvan, V., Wu, Q., and Killeen, T. L.: Mesospheric Doppler Wind Measurements from Aura Microwave Limb Sounder (MLS), Adv. Space Res., 42, 1246–1252, doi:http://dx.doi.org/10.1016/j.asr.2007.06.014, http://www.sciencedirect.com/science/article/pii/S0273117707006412, 2008.

Xia, H., Dou, X., Sun, D., Shu, Z., Xue, X., Han, Y., Hu, D., Han, Y., and Cheng, T.: Mid-altitude wind measurements with mobile Rayleigh Doppler lidar incorporating system-level optical frequency control method, Opt. Express, 20, 15 286–15 300, doi:10.1364/OE.20.015286, http://www.opticsexpress.org/abstract.cfm?URI=oe-20-14-15286, 2012.

Yuan, T., Thurairajah, B., She, C.-Y., Chandran, A., Collins, R. L., and Krueger, D. A.: Wind and temperature response of midlatitude mesopause region to the 2009 Sudden Stratospheric Warming, J. Geophys. Res., 117, D09 114, doi:10.1029/2011JD017142, http://dx.doi.org/10.1029/2011JD017142, 2012.

Zink, F. and Vincent, R.: Wavelet analysis of stratosphere gravity wave packets over Macquarie Island 1. Wave parameters, J. Geophys. Res., 2001.

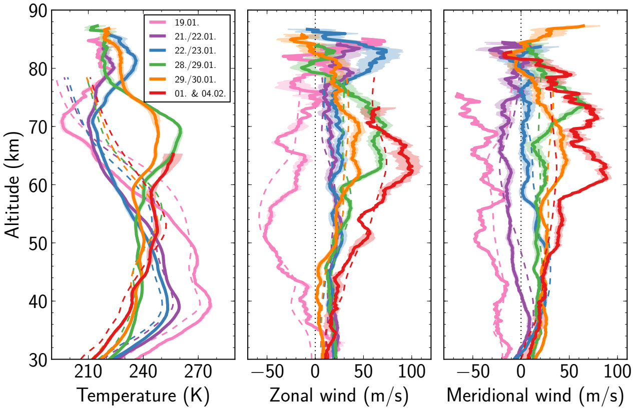

Figure 2. Temporal evolution of temperature and horizontal winds during January and early February 2012 after a minor SSW. The profiles are averages of all 1 h profiles of the respective night(s). Solid lines and shaded areas: lidar data and respective standard deviations; dashed lines: ~~ECWMF~~ ECMWF data with same temporal sampling.

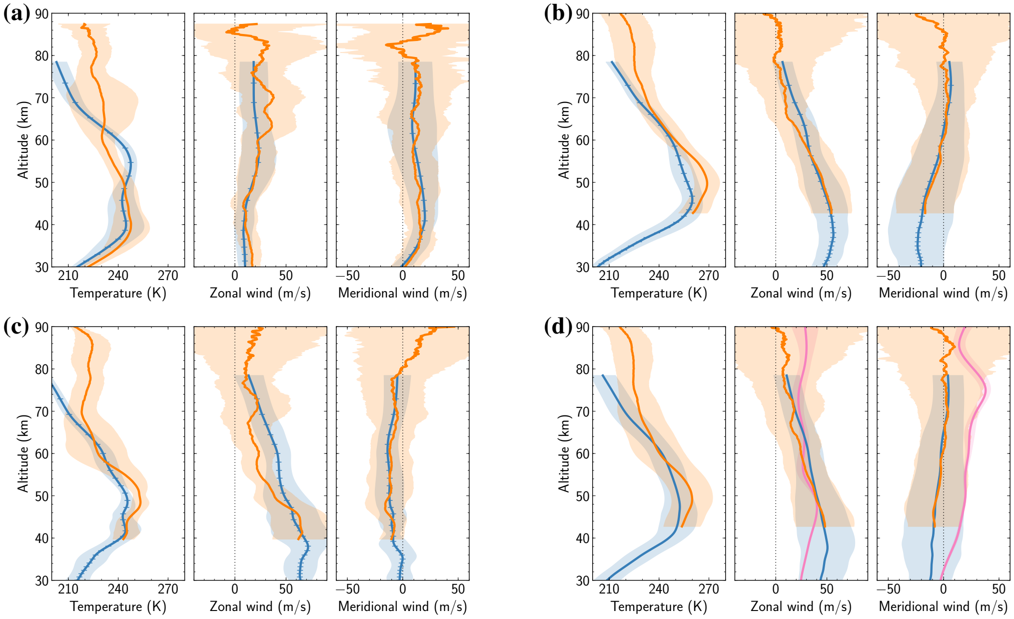

Figure 3. January mean temperatures and horizontal winds for the years 2012 (a), 2014 (b), and 2015 (c), and cumulated data (d). ALOMAR RMR lidar (orange), ECMWF (blue), HWM07 (rose). Shaded areas represent the respective standard deviations. The horizontal bars mark the model levels of ~~ECWMF~~ ECMWF data for one exemplary profile in each season. The ECMWF cycles used are Cy37r3 for 2012 and Cy40r1 for 2014 and 2015.

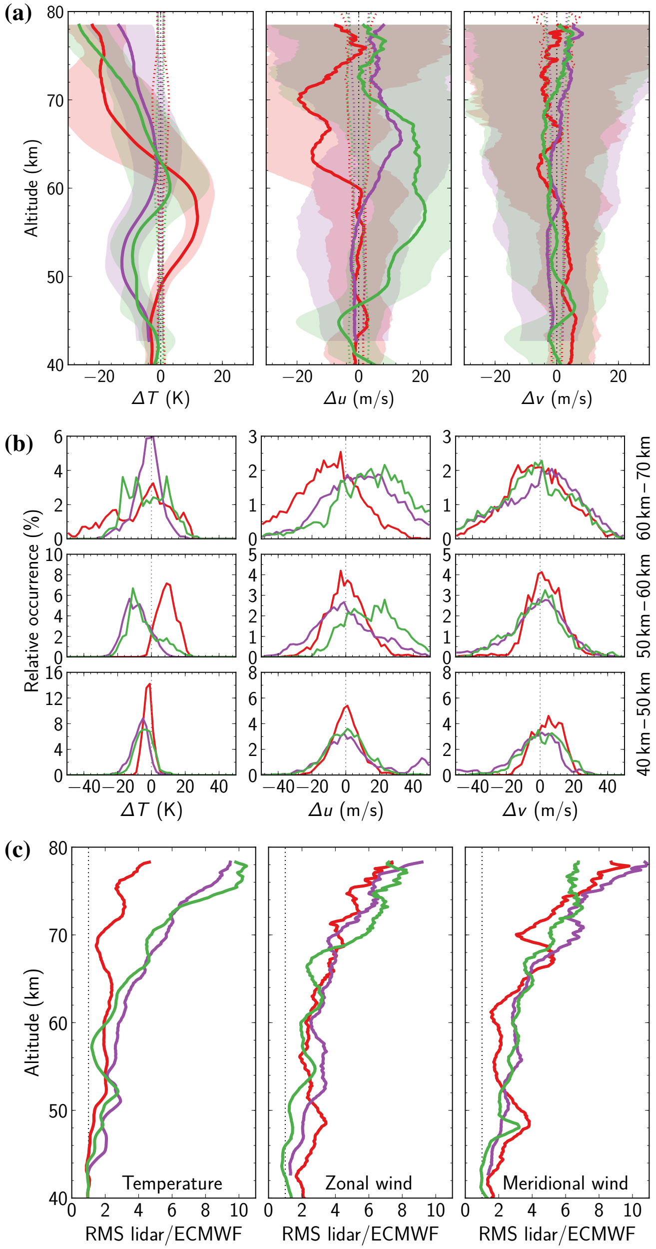

Figure 4. Differences between lidar data and ECMWF data for January 2012 (red), January 2014 (purple), and January 2015 (green)~~.~~; the ECMWF cycles used are Cy37r3 for 2012 and Cy40r1 for 2014 and 2015. **(a)** Mean difference $\frac{1}{N}\Sigma(x_{\mathrm{ECMWF}} - x_{\mathrm{lidar}})$; shading represents the respective standard deviations, dotted lines depict the standard error of the mean of the lidar data. **(b)** Distribution of differences $x_{\mathrm{ECMWF}} - x_{\mathrm{lidar}}$ on hourly basis for different altitude ranges. **(c)** Mean ratio of RMS of lidar and ECMWF data. See Tab. 2 for an overview of the number of 1 h profiles taken into account.

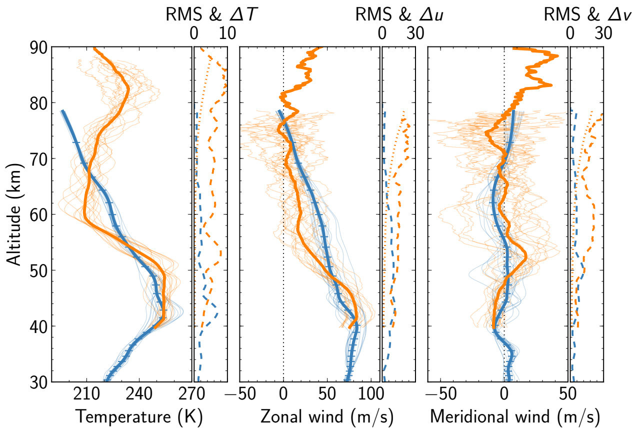

Figure 5. Temperature and horizontal winds for the night 20/21 January 2015; lidar (orange), ECMWF (blue). Thin lines denote 1 h profiles, thick lines denote the ~~night-mean~~ nightly mean profiles, the horizontal bars mark the model levels of ~~ECWMF~~ ECMWF data for one exemplary profile; dashed and dotted lines show the RMS and the mean measurement uncertainty of the 1 h profiles, respectively.

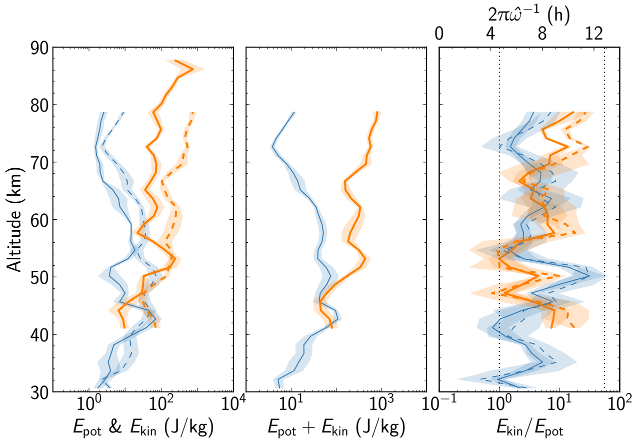

Figure 6. ~~Gravity-wave~~ Gravity wave energy densities per unit mass and the intrinsic period~~of the~~ ($2\pi\hat{\omega}^{-1}$) a monochromatic gravity wave ~~ensemble~~ with the given kinetic-to-potential GWED ratio would have, for the night 20/21 January 2015; lidar (orange), ECMWF (blue). Left: potential (solid) and kinetic (dashed) GWED. Middle: total GWED. Right: kinetic-to-potential GWED (solid) and ~~intrinsic period~~ $2\pi\hat{\omega}^{-1}$ (dashed); the dotted vertical lines denote unity and $2\pi f^{-1}$, respectively. Shading represents the respective standard deviation.

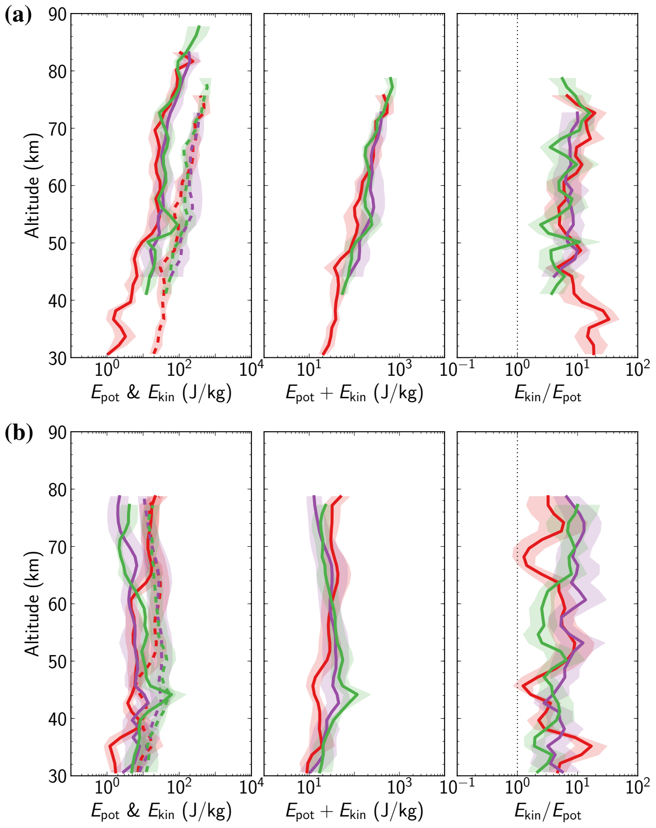

Figure 7. January mean gravity wave energy densities for 2012 (red), 2014 (purple), and 2015 (green) derived from lidar data (a) and ECMWF data (b). Shading represents the respective standard deviation. Left~~panel~~: ~~Potential and kinetic GWED are indicated by~~ potential (solid) and kinetic (dashed~~lines, respectively~~) GWED. Middle: total GWED. Right: kinetic-to-potential GWED.

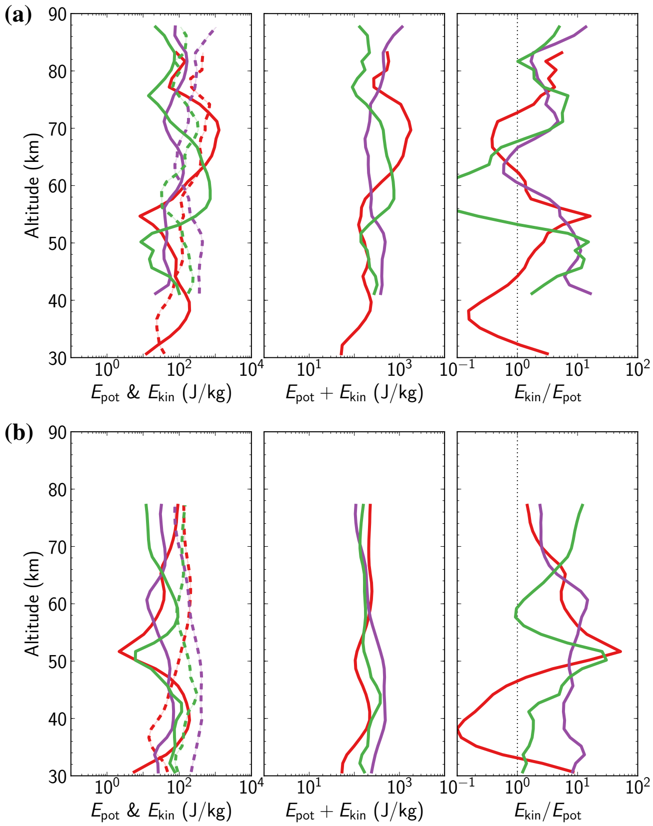

Figure 8. January energy densities per unit mass for large-scale waves for 2012 (red), 2014 (purple), and 2015 (green) derived from lidar data (a) and ECMWF data (b); see text for details. Left: potential (solid) and kinetic (dashed) LWEDs. Middle: total LWED. Right: kinetic-to-potential LWED.

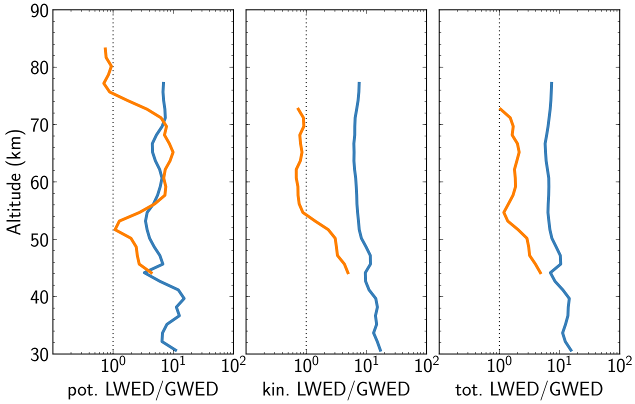

Figure 9. Mean LWED-to-GWED ratios for lidar data (orange) and ECMWF data (blue). Left: potential energy densities. Middle: kinetic energy densities. Right: total energy densities.

Table 1. List of lidar observations taken into account in this study.

night	1 h profiles
19/20 January 2012	2
21/22 January 2012	15
22/23 January 2012	13
23/24 January 2012	2
24/25 January 2012	3
28/29 January 2012	12
29/30 January 2012	15
1/2 February 2012	1
3/4 February 2012	2
10/11 January 2014	14
11/12 January 2014	17
14/15 January 2014	11
15/16 January 2014	17
17/18 January 2014	11
18/19 January 2014	17
19/20 January 2014	13
20/21 January 2014	11
21/22 January 2014	5
22/23 January 2014	12
23/24 January 2014	1
24/25 January 2014	12
26/27 January 2014	10
27/28 January 2014	5
29/30 January 2014	7
30/31 January 2014	7
19/20 January 2015	16
20/21 January 2015	16
21/22 January 2015	13
22/23 January 2015	16
23/24 January 2015	17

Table 2. Number of nights and 1 h profiles taken into account for figures showing ~~month-mean~~ monthly mean data.

year	all observations		long observations (≥ 10 h)	
	nights	1 h profiles	nights	1 h profiles
2012	7	62	4	55
2014	16	170	11	145
2015	5	78	5	~~78~~ 76[a]

[a] The observations in the night 21/22 January 2015 consist of two parts of 11 h and 2 h, respectively, separated by a gap of 5 h.